MULTI-DIMENSIONAL NODALIZATION OF A PRESSURIZED WATER REACTOR CORE USING RELAP5-3D

A Thesis

by

WILLIAM M. COOK

Submitted to the Office of Graduate and Professional Studies of
Texas A&M University
in partial fulfillment of the requirements for the degree of

MASTER OF SCIENCE

Chair of Committee,	Yassin A. Hassan
Committee Members,	Maria King
	William H. Marlow
Head of Department,	Yassin A. Hassan

December 2014

Major Subject: Nuclear Engineering

ABSTRACT

This thesis work involves the use of the RELAP5-3D thermal hydraulic code to model flow for a typical pressurized water reactor (PWR). A model using several three-dimensional components was created to accurately predict complex accident scenarios with greater fidelity and detail than models consisting of only one-dimensional control volumes. In order to build this model, a one-dimensional model was first used as a reference and a foundation. The three-dimensional model was then constructed from this reference model using various techniques and methodologies. These are described in this thesis and represent best practices for similar work. Additionally, a tool was constructed to enhance the ease and accuracy of utilizing both Cartesian and cylindrical components. An overview of this tool is presented in this thesis, which includes verification and validation efforts as well as a discussion on its capabilities and use. After the three-dimensional model had been finalized, it was compared to its one dimensional analogue using a variety of metrics that demonstrate its consistency with the one dimensional reference. A detailed summary of this comparison is presented in this work. The final model was developed for use in Loss-of-Coolant Accident (LOCA) scenarios that simulate hypothesized situations relating to the Nuclear Regulatory Commission's (NRC's) Generic Safety Issue 191 (GSI-191). Thus, a standard of prudence was implemented (i.e. specifications) to ensure the model would be capable of accurately predicting phenomena associated with such scenarios.

ACKNOWLEDGEMENTS

I would like to thank my committee chair, Dr. Hassan, and my committee members, Dr. Marlow and Dr. King for their support during the course of the thesis process and for their advice and guidance towards the completion and finalization of this work. Additionally, I would like to thank Dr. Rodolfo Vaghetto for his mentorship and assistance during the entire process, including the guidance, review, and criticism of the project at various stages of development. I would also like to thank Alessandro Vanni for his help in the development of the three-dimensional RELAP5-3D model. Furthermore, I appreciate the help of Andrew Franklin and Timothy Crook in reviewing the work of the thesis and in resolving some of the issues that were encountered during the modeling process.

I also want to extend my gratitude to the Institute of Nuclear Power Operations (INPO) which awarded me a fellowship for the first portion of my graduate studies and Southern Company, which provided funding through a research assistantship during the second portion of my graduate studies at Texas A&M University.

Finally, thanks to my mother, father, family, and friends for their encouragement, support, and prayers both during my graduate studies and before I entered graduate school.

TABLE OF CONTENTS

Page

LIST OF FIGURES

FIGURE Page

FIGURE Page

FIGURE Page

LIST OF TABLES

1. INTRODUCTION

Nuclear power accounts for a significant portion of the global and domestic supplies of electricity. Worldwide, 435 nuclear reactors are in operation with 72 new nuclear plants under construction as of May 2014 (Knowledge Center, 2014). These reactors accounted for 12.3% of the world's electricity production in 2012. Within the United States, nuclear power accounts for an even greater portion, producing 19.4% of the 2013 U.S. electricity supply. As these facilities continue to operate and develop, safety must be kept paramount. One of the most common design basis accidents for operating light water reactors (LWRs) is a LOCA. Several codes have been developed to simulate the evolution of a LOCA transient. One of the most well accepted family of codes is the Reactor Excursion Leak Analysis Program (RELAP). The decision to utilize the RELAP5-3D version of this program is discussed in the literature review section. In order to fully utilize the capabilities of RELAP5-3D, models of reactors must be as representative of their physical counterparts as possible. This entails the use of three-dimensional nodalization schemes.

A three-dimensional model of a typical four loop PWR (e.g. Westinghouse PWR) was created in RELAP5-3D as part of this thesis work. The model was verified using an analogous one- dimensional model of the same design, referred to as "1D-REF" or "one-dimensional reference" hereafter. This one-dimensional reference model also serves as a foundation, upon which the full three-dimensional model was developed.

Such a model is needed for accurate simulations of complex phenomena and scenarios. This model was developed such that it could be used for LOCA simulations for GSI-191 studies. GSI-191 affects currently operating PWRs in the United States. A discussion on GSI-191 is presented in the literature review section, along with ongoing efforts for its resolution.

Additionally, this thesis outlines the methodologies used in the formation of the RELAP5-3D input deck. The goal of this portion of the work is to discuss lessons learned and propose best practices in the implementation of a RELAP5-3D model using three-dimensional components. A step-by-step description of the development process is provided in the modeling approach section.

As part of the development process, a tool was created to help RELAP5-3D users better implement the code for both accuracy and efficiency. This tool helps to automate and simplify the creation of junctions between RELAP5-3D component control volumes. It was applied in this work for the creation of junctions between adjoining three-dimensional components that were modeled using both cylindrical and rectangular nodalization schemes. Such junctions present a challenge for modelers because they are both time-consuming to generate manually, and human error (such as those caused by estimation) can be introduced into the RELAP5-3D input deck. Additionally, the proposed design process for utilizing three dimensional components involves several iterations of RELAP5-3D models using different nodalizations. Thus, the benefits of such a tool are proliferated due to the inherent repetition of the process. A detailed

discussion on this tool is presented in the multiple junction tool section. This discussion includes tool features, tool implementation, and tool verification and validation (V&V). The tool verification is performed by comparing the tool to analytical solutions, and the tool validation is performed by examination of the results produced by RELAP5-3D models that implemented the tool.

Lastly, the RELAP5-3D results for the three-dimensional model are compared with those of the one-dimensional reference model. The values reported in this thesis are illustrative of the system as a whole. The specific data is organized into two categories: specific reactor parameters and fuel temperatures. These results show that, holistically, the three-dimensional model is consistent with the one-dimensional reference model.

2. LITERATURE REVIEW

The RELAP5-3D code is a state of the art system analysis code used primarily for safety analyses of existing and hypothesized nuclear power plants. RELAP5-3D has been used to model a variety of steady-state and transient system scenarios and is mature and well-understood by the community.

The RELAP5-3D code belongs to a group of computer simulation tools classified as "thermal hydraulic system codes." These codes provide "best estimate" solutions for large, complex problems, such as a nuclear reactor and nuclear steam supply system (NSSS). These codes solve the mass, momentum, and energy conservation field equations for two-phases, and have additional features for more complicated modeling such as that associated with non-condensable gases (Petruzzi & D'Auria, 2008). This group of codes also has the benefit of producing results for both steady-state and transient problems with run times that are acceptable for reactor safety analyses such as a LOCA simulation. The RELAP family of codes has been developed and accepted by the NRC for previous studies (Fletcher, Bayless, Davis, & et.al., 1997). While RELAP5-3D was not directly developed for the NRC, it maintains the legacy from previous versions and is sufficient for most nuclear system transients. The most significant improvement in RELAP5-3D from previous versions is the addition of "…fully integrated, multi-dimensional thermal-hydraulic and kinetic modeling capability" (Idaho National Laboratory, 2014).

The RELAP5-3D code is formally documented in a six volume user's manual available through Idaho National Laboratory to licensed RELAP5-3D users (RELAP5-3D Manuals, 2012). The first volume serves as an overview of the capabilities of RELAP5-3D. It includes a discussion on the structure of the code, the models used in the code, and their implementation towards finding solutions. This volume was used primarily to increase the accuracy and decrease the computational needs of the proposed RELAP5-3D model. The second volume serves as the general user's guide and provides input requirements. The appendix of this volume describes each card that can be used in a RELAP5-3D input deck. This volume was instrumental in building the input deck such that the model most closely resembled the information gathered from the reference and engineering documents. The third volume contains the developmental assessment of the code, and helps build the credibility of the code, while providing reference material to the verification and validation of specific RELAP5-3D models and results. The fourth volume discusses in detail the models and correlations implemented in RELAP 5-3D. The fifth volume provides guidelines and good practices for the code. This volume assisted in the creation of a technique that is efficient and repeatable. Lastly, the sixth volume discusses the numerical scheme implemented in RELAP5-3D.

The need for a comparison of RELAP5-3D capabilities versus the previous one dimensional code, RELAP5-MOD3 is obvious in the work of Roux. In the Roux paper, the cross-flow capability of RELAP5-MOD3 is compared with the results from a computational fluid dynamics (CFD) model using the FLUENT code. The results

illustrate that the RELAP5-MOD3 cross-flow models are insufficient for modeling even single-phase flows with simple geometry (Roux, 2001). Conversely, CFD codes (such as FLUENT) are not capable of modeling the full reactor system due to computational limitations. This is a prime example of the niche that RELAP5-3D fills. By using a three dimensional nodalization, the thermal hydraulics of real systems can be better modeled. In this scenario, a three-dimensional nodalization could be used to explicitly model flow in the lateral direction, without having to rely on a correlation or a correction factor. This thesis adds to the body of knowledge with respect to the capability and implementation of three dimensional system codes to model real problems.

An actual comparison of a one dimensional model and a three dimensional model was performed by the RELAP5-3D development team (Idaho National Laboratory, 2014). In this report, both models were compared with experimental data from the LOFT Test L2-5. These comparisons included both the calculation of initial conditions, and the timings of several events during the experiment. The final results of this study indicated that both models share similar predictions for loop behavior, since three dimensional models were only used in the reactor vessel. While both models were "generally in reasonable agreement" with the test, the three dimensional model's results were "generally as good as or better than" the results of the one dimensional model.

The sensitivity of RELAP5-3D was studied in numerous works using the DAKOTA code (Rodriguez, 2012), (Magnusson, 2013). These studies have helped to

illustrate how the RELAP5-3D output is affected by the user's input. With this information, better models can be developed using more appropriate input parameters.

Verification and validation of RELAP5-3D is ongoing, but very mature (RELAP5-3D Manuals, 2012). In addition to the phenomenological, separate effects, and integral effects cases documented in volume 3 of the RELAP5-3D manual, many independent benchmarks have been completed with mostly positive results. For example, a one-dimensional model has been tested against the PREMIUM benchmark based on experiments performed at the FEBA facility in Germany with mostly "satisfactory" agreement to the benchmark (Magnusson, 2013). Three-dimensional models have also been successfully benchmarked. For example, a three-dimensional nodalization was used to compare RELAP5-3D simulations with the BFBT benchmark organized by OECD-NEA, the NRC, and NUPEC of Japan (Kovtonyuk, Petruzzi, Parisi, & D'Auria, 2008). This study also showed the ability of RELAP5-3D to successfully model many of the thermal hydraulic properties of interest. The results of these studies illustrate the maturity of the RELAP5-3D code and its applicability to the thermal hydraulics of nuclear power plants.

The model developed as part of this thesis was intended for use in efforts to resolve GSI-191. This issue seeks to determine if the operation of the Emergency Core Cooling System (ECCS) is at a risk for failure following a PWR LOCA. In the event of a LOCA, debris may be generated from piping insulation and other materials within the containment. The transport and accumulation of this material may lead to safety issues.

For example, this debris may accumulate on the recirculation (emergency) sump screen, resulting in head loss for the ECCS or containment spray (CS) pumps (Los Alamos National Laboratory, 2002). This debris may be transported further, causing damage to these pumps, or it may be transported into the reactor coolant system (RCS), itself. This debris could cause channel blockage or other effects within the RCS. The model developed in this thesis is designed to model such events, especially events that may be dependent on three-dimensional flow within the reactor vessel.

3. MODELING APPROACH

This thesis involves three main steps: the formation of an appropriate RELAP5-3D input deck, the creation and documentation of a tool that increases accuracy and efficiency of the modeling approach, and detailed analysis of the final RELAP5-3D steady-state results and comparison of these results to the one-dimensional reference model. This section focuses on the first of these three topics.

3.1. One-Dimensional Model

In order to assure the quality of the model, a suitable 1D RELAP5-3D reference model was utilized. This reference model conforms to typical plant operating conditions. This model will serve as a good benchmark to judge the representativeness of the 3D model to actual power plants without having to find plant-specific data, which may vary from the RELAP5-3D predictions due to uncertainties within the code and the measurement or calculation of parameters.

Before discussing the steps that went into the creation of the three-dimensional model, a background description of the one-dimensional model is useful. The one-dimensional model consists of 4 loops and a reactor vessel, with loop 4 possessing a pressurizer. The nodalization of the one-dimensional model is provided in Fig. 3.1. All four loops are composed of a hot leg, a steam generator, a crossover leg, a reactor

coolant pump (RCP) and a cold leg. Each steam generator is modeled with a primary side and a secondary side, with heat structures (representing u-tubes) coupling the two. These RCS legs were unchanged during the conversion of the model from only one-dimensional components to a mixture of both one-dimensional and three-dimensional components. This modeling decision was chosen due to the purpose of the final model. There are no hypothesized events associated with GSI-191 studies that would require three-dimensional spatial fidelity in the RCS legs beyond what is already provided by the one-dimensional nodalization.

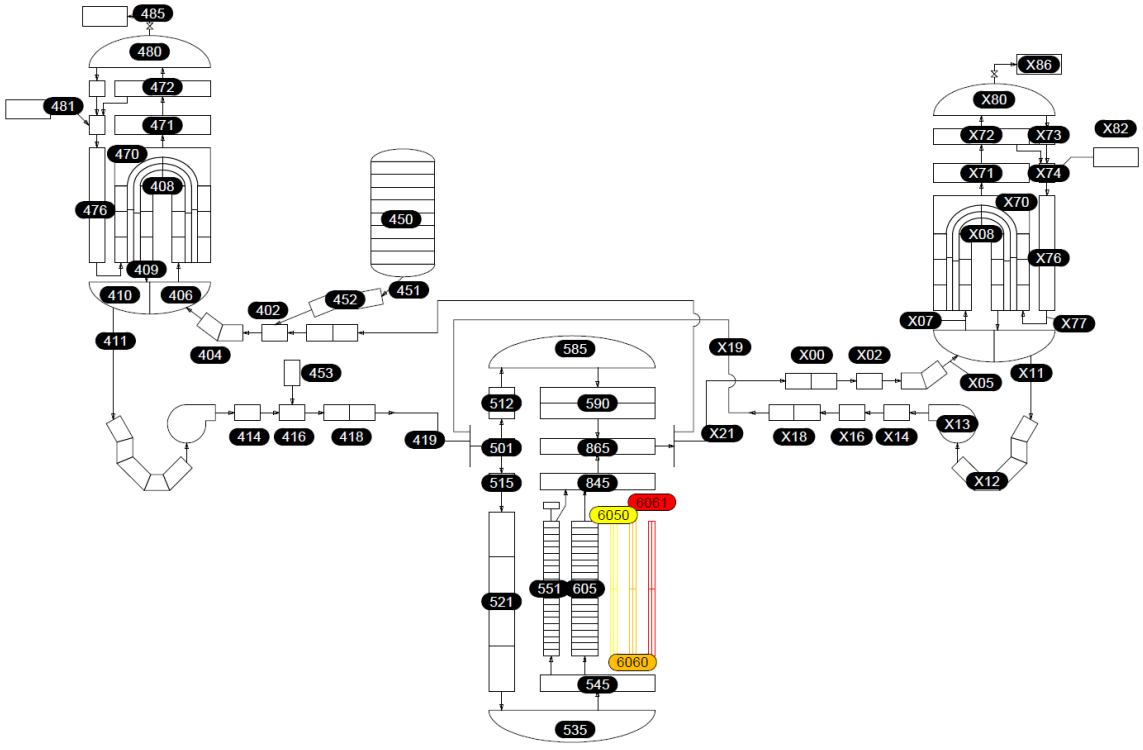

Figure 3.1. RELAP5-3D nodalization of the one-dimensional reference model.

While the four RCS legs of the one-dimensional model will remain unchanged, the nodalization within the reactor vessel will be changed to suit the needs of GSI-191 studies. The one-dimensional model consists of several volumes within the reactor vessel. Each of the four cold legs is connected to a single "vessel entry" region (501). From here, the flow branches into two paths. The first path represents the "upper bypass" flow. This flow path consists of nodes 512, 585, and 590. This flow path will also remain unchanged for the reasons previously mentioned.

The second path from the core entry annulus consists of the downcomer (515 & 521), the lower plenum (535), the lower core plate region (545), the core bypass (551), the reactor core (605), the upper core plate region (845), and the vessel exit region/ upper plenum bottom (865). All of these components except the core bypass will be converted from one-dimensional nodalizations to three-dimensional nodalizations. While the core bypass will remain one-dimensional, its nodalization will be updated to fit well with the three-dimensional components. This is discussed in more detail in section 3.5.

The core region is coupled with heat structures representing nuclear fuel. Heat structure 6050 represents the effects of all assemblies lumped together with the exception of the hottest assembly. Heat structure 6060 represents only the hottest assembly, while heat structure 6061 represents the hottest rod from the hottest assembly. These representations are helpful in modeling reactor accidents, since they provide

important safety data. In the three-dimensional model all 193 fuel assemblies are modeled individually.

3.2. First Iteration Three-Dimensional Model

The starting point of the modeling approach was to make 3D analogues of certain 1D components within the reactor vessel. The components chosen to be modeled using a 3D nodalization were the vessel entry, vessel downcomer, lower plenum, lower core plate, reactor core, upper core plate, and vessel exit. Components that model the vessel upper plenum and core bypass were maintained as 1D components to decrease computation time, while having little influence on the desired results during hypothetical LOCA sequences associated with GSI-191. This decision is consistent with a previously published three-dimensional PWR model; this model will be referred to as "3D-REF" or "three-dimensional reference" hereafter (Vaghetto & Hassan, 2013). The components that were transformed into three-dimensional analogues were chosen based on the expectation of complex coolant flow paths during an accident simulation. These flows could be affected by problem asymmetry due to several factors such as blockage of channels or the spectrum of spatial points that could act as sources or sinks (injections or leaks) of coolant. Additionally, the ability for flow to be explicitly modeled in three-dimensional space may be of importance in these regions during an accident scenario in order to ensure that mass, momentum, and energy are transported in ways that are as

physically accurate as possible. This is consistent with the RELAP5-3D program summary which states that three-dimensional nodalization is "typically [used to model] the lower plenum, core, upper plenum, and downcomer regions of an LWR" (Idaho National Laboratory, 2014).

Decisions on initial mesh sizes and component selection were made in part based on the modeling approaches of both the one-dimensional and three-dimensional reference models. These decisions were revisited later based on analysis of the steady state predictions of RELAP5-3D. This process was designed to eliminate any problems that may cause the RELAP5-3D simulation to not run correctly. These problems included geometry and closure errors, typographical and format errors in the input deck, and errors that led to instabilities in the modeled flow. Additionally, since systems codes are sensitive to nodalization decisions, some nodalizations may yield non-physical results.

In order to make three-dimensional analogues, a prioritization scheme had to be created when modeling conflicts arose. The priority for input parameters from highest to lowest was (1) elevation change, (2) component volume, (3) junction flow area, (4) hydraulic diameter, (5) component flow area, (6) flow length, and (7) junction flags and models. Parameters with lower numbers were maintained at values equivalent to the one-dimensional reference values when conflicts arose. Under certain conditions, this priority was shifted to ensure the holistic model exhibited similar behavior to the 1D reference, even if slight changes to certain components were necessary.

An example of a change that occurred when the model was transitioned from only 1D components to the 3D components occurred in the vessel lower plenum. Due to the limitations of the one-dimensional functionality, the 1D lower plenum was modeled as a "branch" component consisting of a single geometric dimension, and a few scalar quantities, such as flow area and pipe roughness. When the lower plenum was modeled as a three dimensional, "multid," component, a shape should be assumed or derived from engineering sketches and documents. The first step in the design of the lower plenum component was the axial length and number of nodes. The lower plenum was modeled as two axial disks, with each disk having one-half of the original 1D-axial length. This length corresponds to the component height and elevation change. The upper disk was assigned the component identification number 535, while the lower disk was assigned the number 525. Since the axial dimension is equivalent to its 1D model analogue, the average cross-sectional area of the two disks must also be equivalent in order to preserve the total volume of the lower plenum. Additionally, the outer radius of the downcomer region must be equivalent to the outer radius of the top node of the lower plenum. With these constraints, the inner radius of the downcomer region was taken to be equivalent to the radius that corresponds to a circle with area equivalent to the average cross-sectional area of the lower plenum. This is shown in Fig. 3.2.

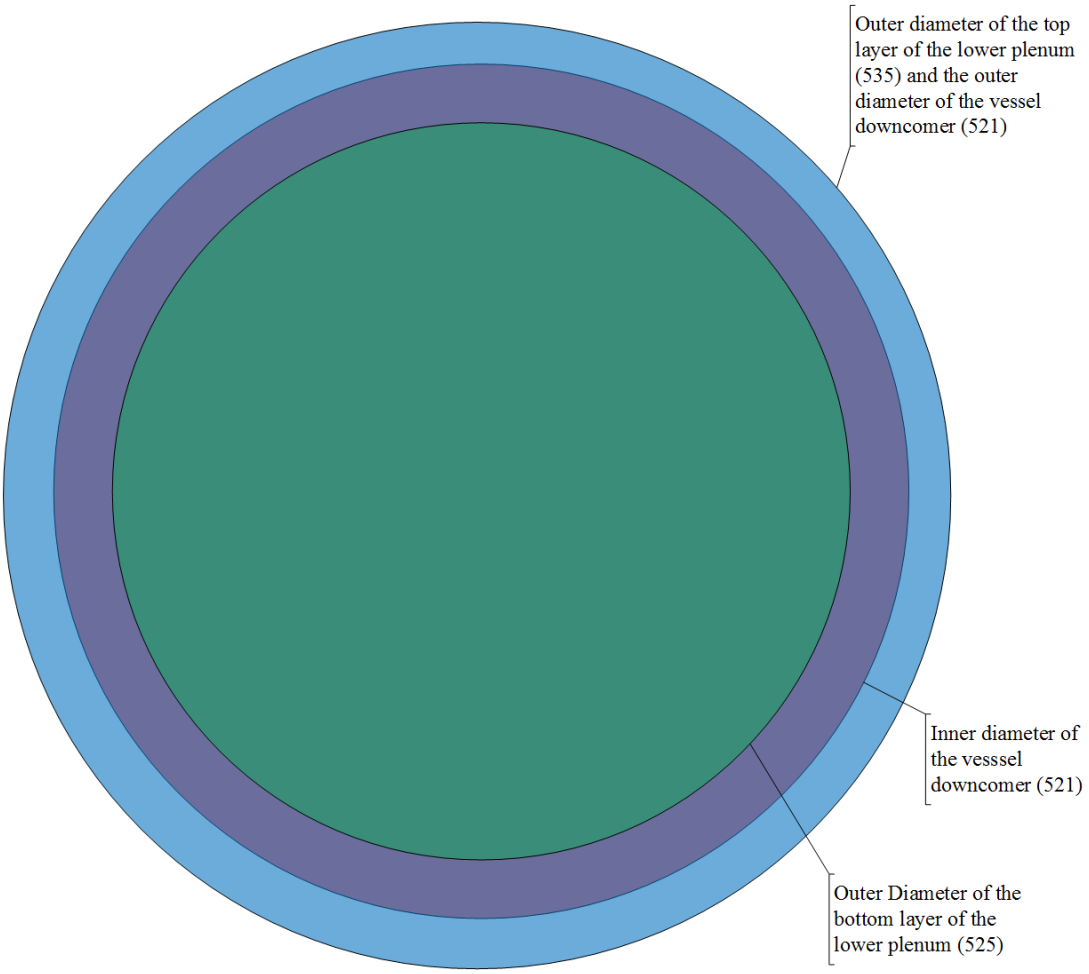

Figure 3.2. Relationships between the diameters of the three-dimensional downcomer and lower plenum.

This nodalization resulted in the upper disk (535) containing 63.54% of the total volume, while the lower disk (525) contained 36.46%. By comparison, the 1D model was limited to 50% volume in each equivalent node, while a perfect hemisphere results in 79.69% of the volume in top half and 20.31% in the bottom half.

In addition to satisfying the physical considerations, the three-dimensional modal must satisfy the geometry closure requirements of the RELAP5-3D code (RELAP5-3D Manuals, 2012). These requirements dictate that all control volumes must be defined with Cartesian or cylindrical coordinates that result in spatial conservation around any loop (i.e. any flow path that begins and ends with the same control volume must result in a displacement of approximately zero). It is because of this fact that some of the components had to be redesigned from their one-dimensional analogues. These components were the vessel downcomer and the upper core plate region. Both of these components were modeled as "pipes" that had elevation changes that were less than their flow lengths, with the program still modeling these pipes as vertical. While this is an option for one-dimensional hydrodynamic components, it violates the closure requirements of the three-dimensional components. A number of possible solutions were originally proposed, such as modeling each component with multiple nodes that transition from positive angular orientation to negative angular orientation, such that the inlet and outlet of the component have the correct displacement, but all positions within the component are shifted laterally, thus increasing flow length. This method was attempted, but could not be successfully implemented, as RELAP5-3D continued to have closure errors due to the artificial rotation. With this in mind, the best solution was deemed to be taking the elevation change as the component length, maintaining component flow area, and recovering the lost volume in one-dimensional components elsewhere in the reactor vessel. These two one-dimensional components were the core

bypass and the vessel upperdome. Due to this decision, the downcomer volume was reduced by 4.4% and the upper core plate volume was reduced by 39.4%, while the upper plenum volume was enlarged by 4.2% and the core bypass volume was enlarged by 99.2%. The total volume of the system as a whole was unchanged. The impact of these changes on the final results was deemed acceptable. The increase of flow length in the core bypass added other modeling benefits that will be discussed later.

The nodalization of components within the reactor vessel is summarized in Table 3.1 for the one-dimensional reference model, while the nodalization for the same components in the three-dimensional model is presented in Table 3.2. These tables show the component numbers that define each physical component or region in the RELAP5-3D input deck. When more than one component is used to model the same region, the data for each component is kept separate from the other by a comma in the table. These tables illustrate the increased fidelity and resolution of the three-dimensional components when compared to one-dimensional analogues. In these tables, the number of junctions assigned to a region is equivalent to the sum of the number of junctions between volumes *within* the component and the number of junctions originating *from* the tabulated component *to* another component. While the core plates actually consist of 225 control volumes each and the reactor core actually consists of 2475 control volumes for the three-dimensional nodalization, only those volumes which are used in the RELAP5-3D simulation are tabulated. Additionally, Table 3.2 states that the core bypass region consists of a single node along the lateral axes, however these components

are one-dimensional, with this label added for consistency. The total number of axial nodes for the reactor core was decreased from the one-dimensional model to the three-dimensional model to save on computational requirements while maintaining the integrity of the final intended applications of this model. If the applications of this model were to change, then this value could easily be changed, as well. Lastly, Fig. 3.3 is provided to illustrate the changes to the reactor vessel nodalization. This figure can be compared to the nodalization of the one-dimensional reference model presented in Fig. 3.1 The three-dimensional model also features a heat structure for each axial array of reactor core nodes (i.e. 193 heat structures). The connections to the cold leg occur on the outer face of four nodes of the top layer of 515, and the hot leg connections occur on the outer face of four nodes of the outermost ring of 865.

Table 3.1. A summary of the nodalization of the one-dimensional model for regions that underwent three-dimensional transformations.

Region Name	Component Number(s)	# of Nodes (z)	# of junctions
Vessel Entry	501, 515	1, 1	2, 1
Downcomer	521	4	4
Lower Plenum	535	1	2
Lower Core Plate	545	1	2
Core Bypass	551	22	22
Reactor Core	605	21	21
Upper Core Plate	845	1	2
Vessel Exit	865	1	2
TOTAL	-	51	55

Table 3.2. A summary of the nodalization of the three-dimensional model for regions that underwent transformations from the one-dimensional reference model.

Region Name	Component Number(s)	# of Nodes (x or r)	# of Nodes (y or θ)	# of Nodes (z)	# of Nodes (total)	# of junctions (total)
Vessel Entry	515	1	16	2	32	64
Downcomer	521	1	16	10	160	320
Lower Plenum	525, 535	7, 8	16	1, 1	240	860
Lower Core Plate	545, 546, 547, 548	7, 8, 7, 8	7, 7, 8, 8	1	193	193
Core Bypass	550, 551	1, 1	1, 1	1, 12	13	28
Reactor Core	605, 606, 607, 608	7, 8, 7, 8	7, 7, 8, 8	11	2123	6043
Upper Core Plate	845, 846, 847, 848	7, 8, 7, 8	7, 7, 8, 8	1	193	503
Vessel Exit	865	6	16	1	96	260
TOTAL	-	-	-	-	3050	8271

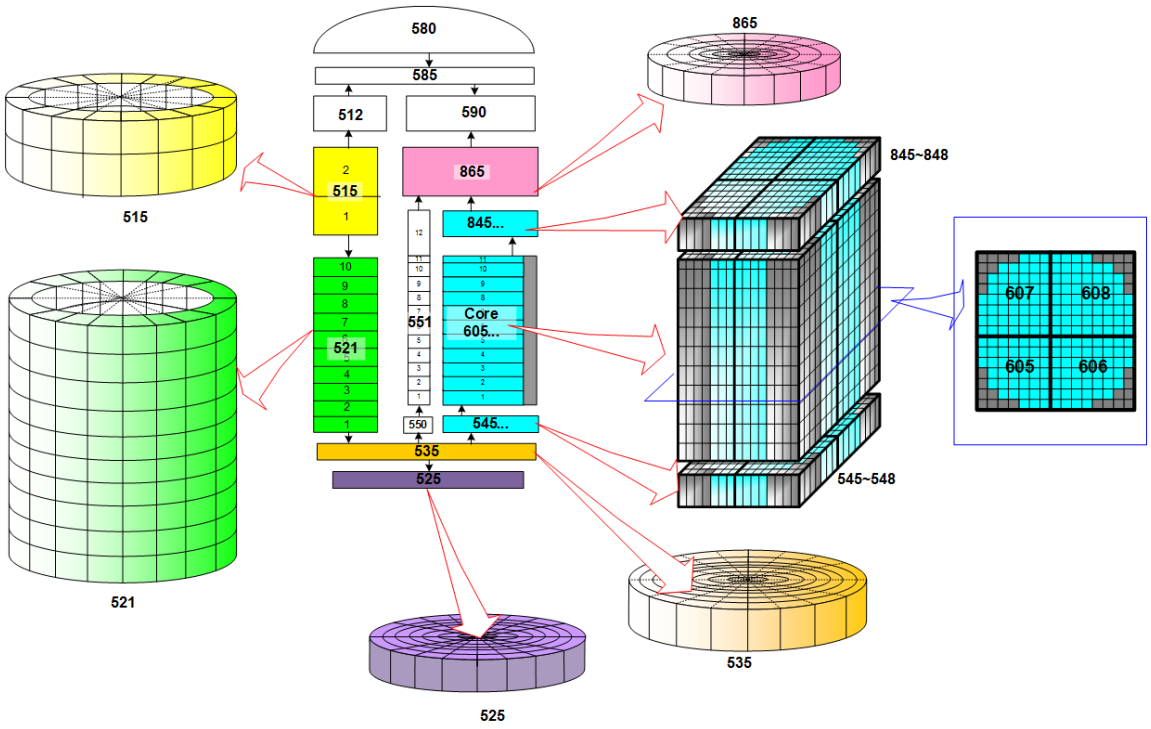

Figure 3.3. Nodalization of the reactor vessel for the three-dimensional model.

After this initial deck was finished, it was checked for consistency with the one-dimensional reference model. In addition to the consistency sought in the input deck of the three-dimensional model, the results should also exhibit very similar behavior to the one dimensional reference, especially during steady-state simulations. Later stages in the modeling approach will be based on this principle.

3.3. Optimization of the Model for Computational Time

The next step in the proposed methodology for model development involves changing the three-dimensional nodalization to more efficiently use computer resources and save on computational and run times. One of the major benefits of this optimization is that it enables users to run more cases within a given timeframe, since each case requires less time to run. It makes sense to perform this step early in the model development process due to the fact that this nodalization will serve as the basis for many other simulations that ensure consistency with the 1-D reference model and hence consistency with physical systems.

The reduction of computational time was accomplished by two principal methods. The first method is to reduce the number of nodes and junctions that have little influence on the results. The second method is to change the nodalization to increase the Courant time step. These two methods involve changing the size and number of control volumes that form components but do not change any physical or geometrical properties of the components themselves.

3.3.1. Time Reduction by a Reduction in the Number of Nodes

The first method to achieve faster simulations is to reduce the total number of control volumes and junctions used to model the problem. When implementing a three-

dimensional nodalization, a single component may be allocated several control volumes and junctions. It is important to only allocate control volumes and junctions that will have an influence on the thermal hydraulic behavior of the system and hence the simulation results.

The RELAP5-3D program utilizes a "scalar node" at the center of each control volume, in order to simulate transport of mass and energy in the system, while it uses a "vector node" at every junction to simulate momentum transport (RELAP5-3D Manuals, 2012). Figure 3.4 has been reproduced from the first volume of the RELAP5-3D manuals. This helps to illustrate the nodalization technique of the program. The semi-implicit scheme implemented in the RELAP5-3D code enables the field equations to be represented as a single difference equation per fluid cell. This results in an N by N system of equations, where N is the number of nodes. This system of equations is solved at every time step, thus a reduction in the number of nodes by one-half reduces the number of equations solved at each time step by 75%, which, in turn, reduces the computational time.

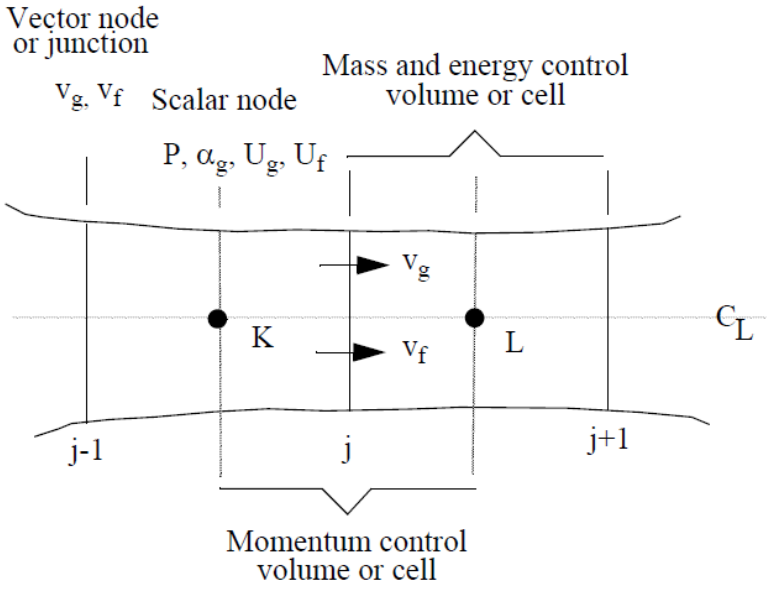

Figure 3.4. Nodalization technique used for the RELAP5-3D equation solver.

To illustrate how the total number of control volumes and junctions can quickly rise for three dimensional components consider the transition of a one-dimensional "pipe" component consisting of 2 control volumes, 2 external junctions, and 1 internal junction. As a three dimensional component, this could be modeled as a cylindrical "multid," consisting of 4 radial rings, 16 angular intervals, and 2 axial volumes. This component would result in the creation of 128 control volumes, 48 internal junctions, and an unspecified number of external junctions. It would be anticipated, based on the discussion above, that the RELAP5-3D program would be forced to solve a factor of approximately 4,000 more equations at every time step, greatly increasing computational time and costs. Figure 3.5 depicts actual and predicted normalized computer run times

for various "steady-state" RELAP5-3D models used in the design process. The abscissa starts with the 1D reference model values, with an additional three-dimensional component being added as the clustered bars move from left to right. The ordinate direction indicates the amount of computational time, $cput$, used per unit time of the simulation, $simt$. The predicted values for each model were based on the number of control volumes, cv, and the number of junctions, jn, as shown by Eq. 3.1, where C is a constant (approximately $6.2*10^{-7}$) obtained by fitting results from a series of RELAP5-3D simulation results. In practice, this constant would be dependent on available computational resources, as well as the model itself. Equation 3.1 was postulated as a reasonable relationship, but is not exact due to the large number of computational demands from other processes and the number of momentum conservation implementation options available to RELAP5-3D users. Table 3.3 provides information on the number of nodes and junctions used in each model, as well as the actual and predicted values of normalized computer run time.

$$\frac{C}{\frac{2}{3}(cv)^2 + \frac{1}{3}(jn)^2} = \frac{cput}{simt} \tag{3.1}$$

Table 3.3. Values for actual and predicted normalized computer run times for several models with differing numbers of control volumes and junctions.

Components Added from Previous Model	cv	jn	actual normalized computer run time	predicted normalized computer run time
1D Model	210	219	0.063	0.028
+ 3D Downcomer	396	612	0.211	0.142
+ 3D Lower Plenum	635	1235	0.444	0.482
+ Extended Bypass	626	1273	0.291	0.497
+ 3D Core Plates	721	1622	0.366	0.759
+ 3D Upper Plenum	1105	2886	1.248	2.226
+ 3D Core	3207	8712	14.348	19.937

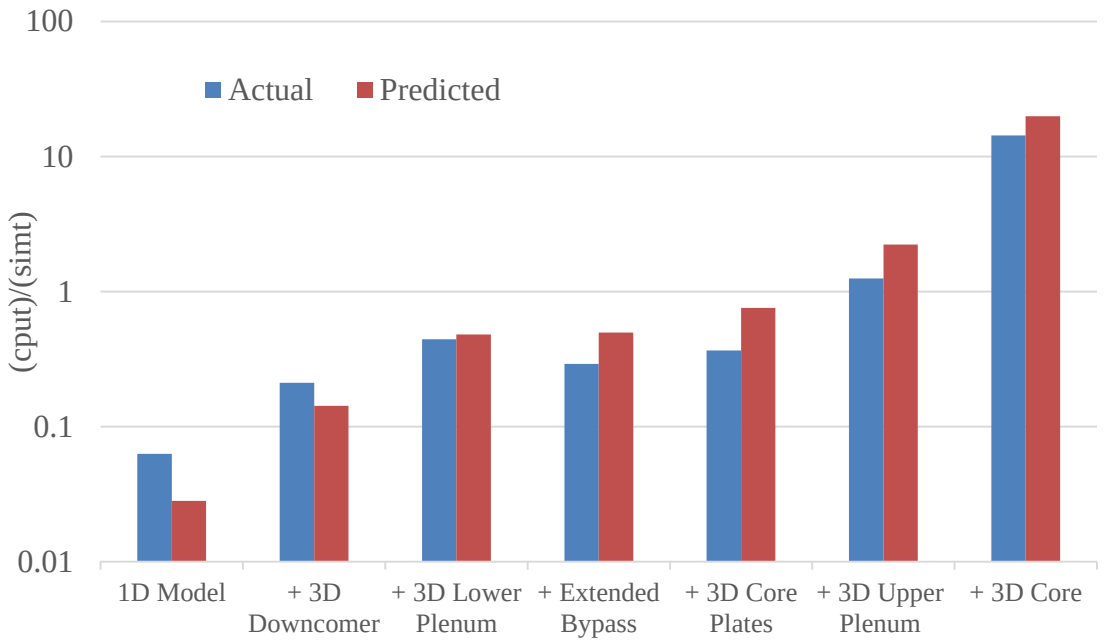

Figure 3.5. Plot of the actual and predicted computer run times for different models.

3.3.2. Time Reduction by an Increase in the Courant Time Step

Another method to reduce total computational time is to increase the Courant time step. The Courant time step is determined by the amount of time it takes for fluid to flow through a limiting node during the simulation. Nodes that have high fluid velocities but short flow lengths result in short material Courant limits. The shortest Courant limit is approximately the same as the time step when the program implements its semi-implicit numerical scheme. Thus, a single poorly designed node or region can cause the entire simulation to run slowly. In fact, according to Volume II of the RELAP5-3D manual, the first "rule" of hydrodynamic nodalization is that "the length of volumes should be such that all have similar material Courant limits…" (RELAP5-3D Manuals, 2012).

A helpful feature of the RELAP5-3D output deck is the inclusion of a table that tallies the number of times a specific node sets the minimum Courant limit for the simulation. In order to increase the Courant time step, a RELAP5-3D input deck was initially run. The corresponding output file was then utilized to identify deficient areas in the nodalization. The nodalization of these areas would be adjusted in a new input deck, and this process would be repeated until a satisfactory solution was produced. In the initial nodalization of the model produced in this thesis, the nodes of the vessel exit region had very small Courant limits in comparison to the rest of the model. After the adjustments and tunings discussed here were implemented, the last axial nodes of the

core usually set the Courant time step, with the vessel entry region occasionally setting the limit, as well.

A depiction of the improvement in computational time as the Courant time step was increased is presented in Fig. 3.6. The selected data points represent different iterations of the same design.

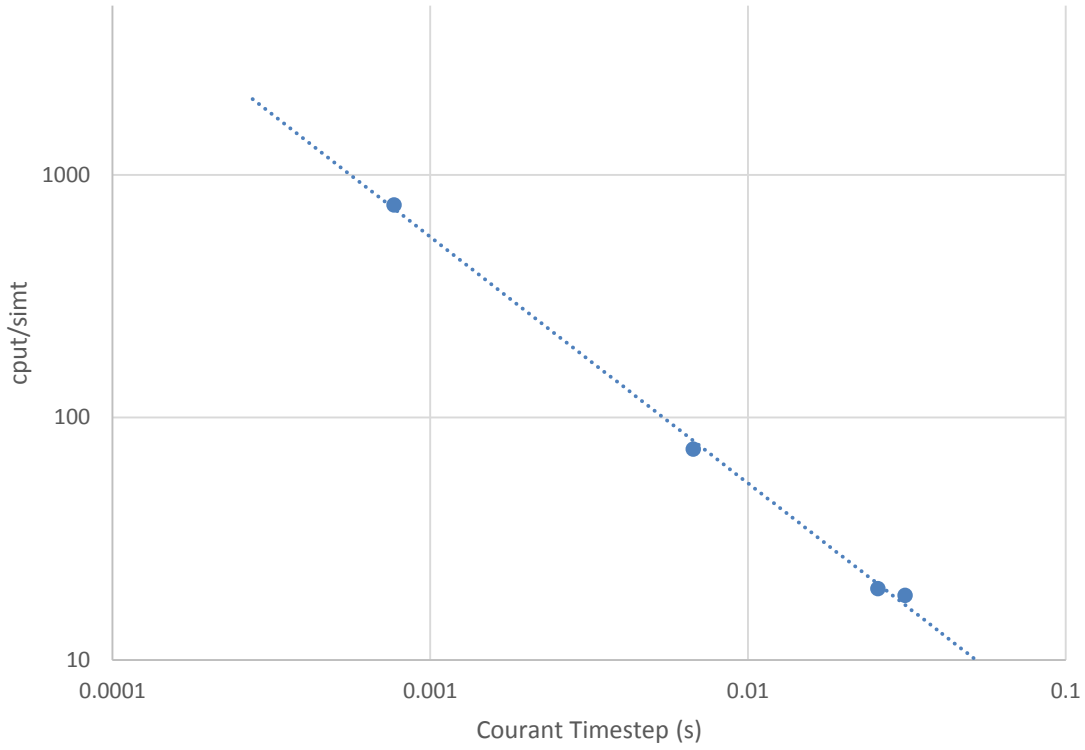

Figure 3.6. Plot of normalized computer run time versus the final Courant timestep.

3.4. Improvements in Model Geometry

After a computationally efficient version of the model was obtained, the nodalization of the design underwent modifications to ensure that the three dimensional components represented a PWR as closely as possible. For example, the design of the three-dimensional components within the reactor vessel was changed to be spatially consistent with the physical arrangement of the RCS loops. The chosen PWR design includes four cold legs and four hot legs, similar to the geometry shown in Fig. 3.7 (Todreas & Kazimi, 2012). Since RELAP5-3D models junctions between volumes as occurring at the center of a specified "face," the corresponding nodalization of the vessel entry and vessel exit regions must have control volumes that are centered at the leg connection locations. The chosen nodalization for the vessel entry and exit, as well as all cylindrical components, utilized 16 angular sectors, encompassing 22.5°, each. This geometry is consistent with each leg being located halfway between its neighboring legs.

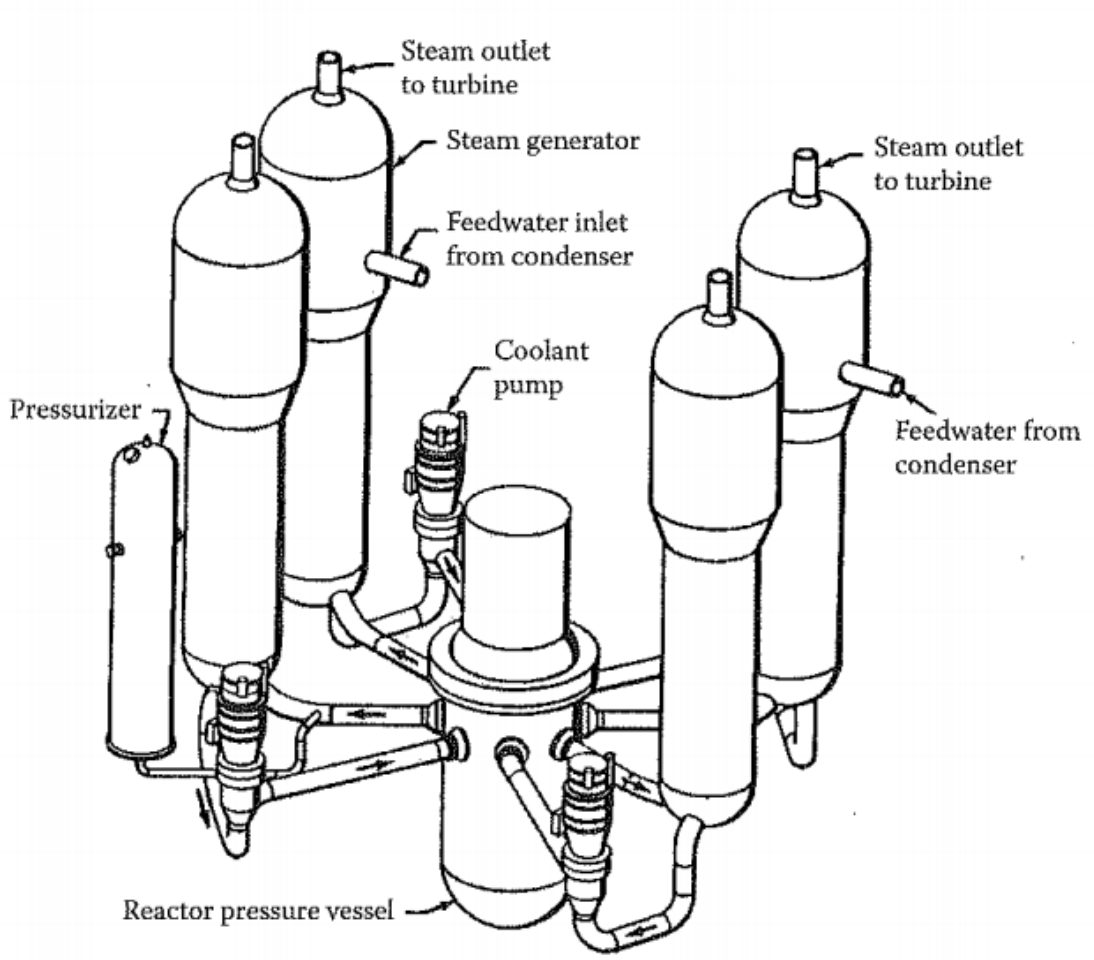

Figure 3.7. Illustration of a typical 4-Loop pressurized water reactor.

Another constraint for the nodalization is vessel symmetry in "quarters" or "quadrants." This means that if the vessel were divided into four equal regions in the (x,y) or (r,θ) planes, then each quarter would be the same, exposing the fluid to identical flow paths, heat structures, and conditions. In order to accomplish this, some of the three dimensional components needed to be rotated to preserve symmetry. Specifically,

all cylindrical components were rotated 11.25°, while the rectangular components were not rotated. This resulted in the necessary symmetry throughout the vessel, and more closely models actual PWR designs. A "top-down" view of the cylindrical and rectangular components is provided in Fig. 3.8 before this rotation took place and in Fig. 3.9 for after this rotation was added. Additionally, Fig. 3.10 and Fig. 3.11 illustrate the peak cladding temperatures of the 193 fuel channels for both the pre-rotation and post-rotation models, respectively. It was expected that the lateral temperature profile for the rotated case would result in more symmetry and uniformity than in the case without rotation. While the results are consistent with this expectation, the effects of not having rotated components is small. While this is true for the steady-state case presented here, it may not be true for more complicated simulations. An example of a situation would be flow blockage of certain fuel channels. This situation may arise during the course of work for the resolution of GSI-191. While both models yield similar results, the rotated version is kept because it represents a more conservative and physically appropriate model, with increased certainty due its geometrical similarity with typical PWRs.

Lastly, the pressure and mass flow through four symmetric fuel channels was compared, as provided in Table 3.4. This table shows the pressure and mass flow at the entry and exit of the fuel channel, as well as the difference from entry to exit, and the absolute deviation of this difference from the mean difference. Figures 3.8 and 3.9 can be used to relate the fuel channel position with respect to the four RCS legs, and Fig. 4.2 can be used to find the exact location of the fuel channels.

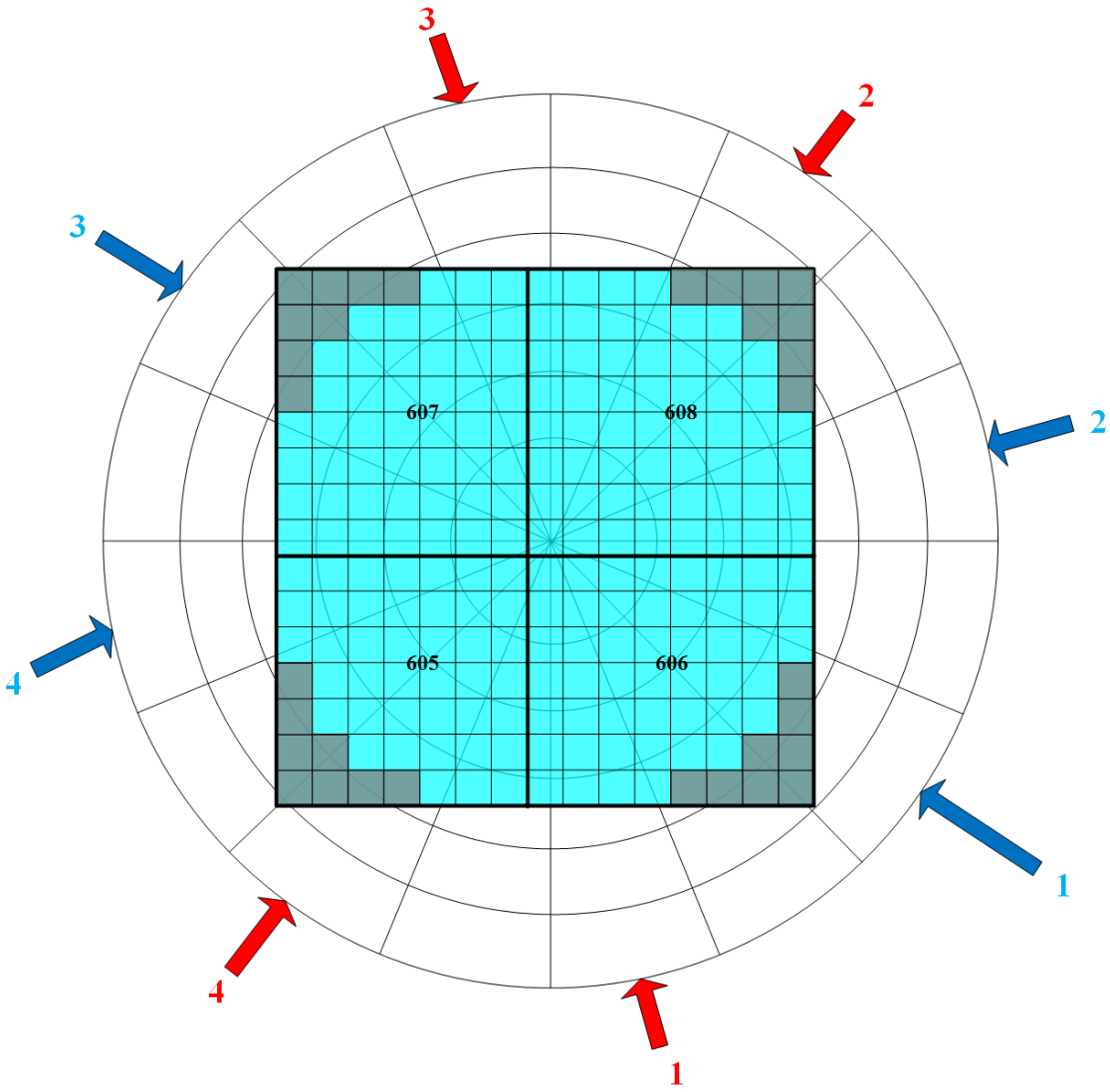

Figure 3.8. Illustration showing an overlay of the Cartesian geometry of the core along with the cylindrical geometry of the plena and the corresponding hot leg (in red) and cold leg (in blue) junctions before any rotation of cylindrical components took place.

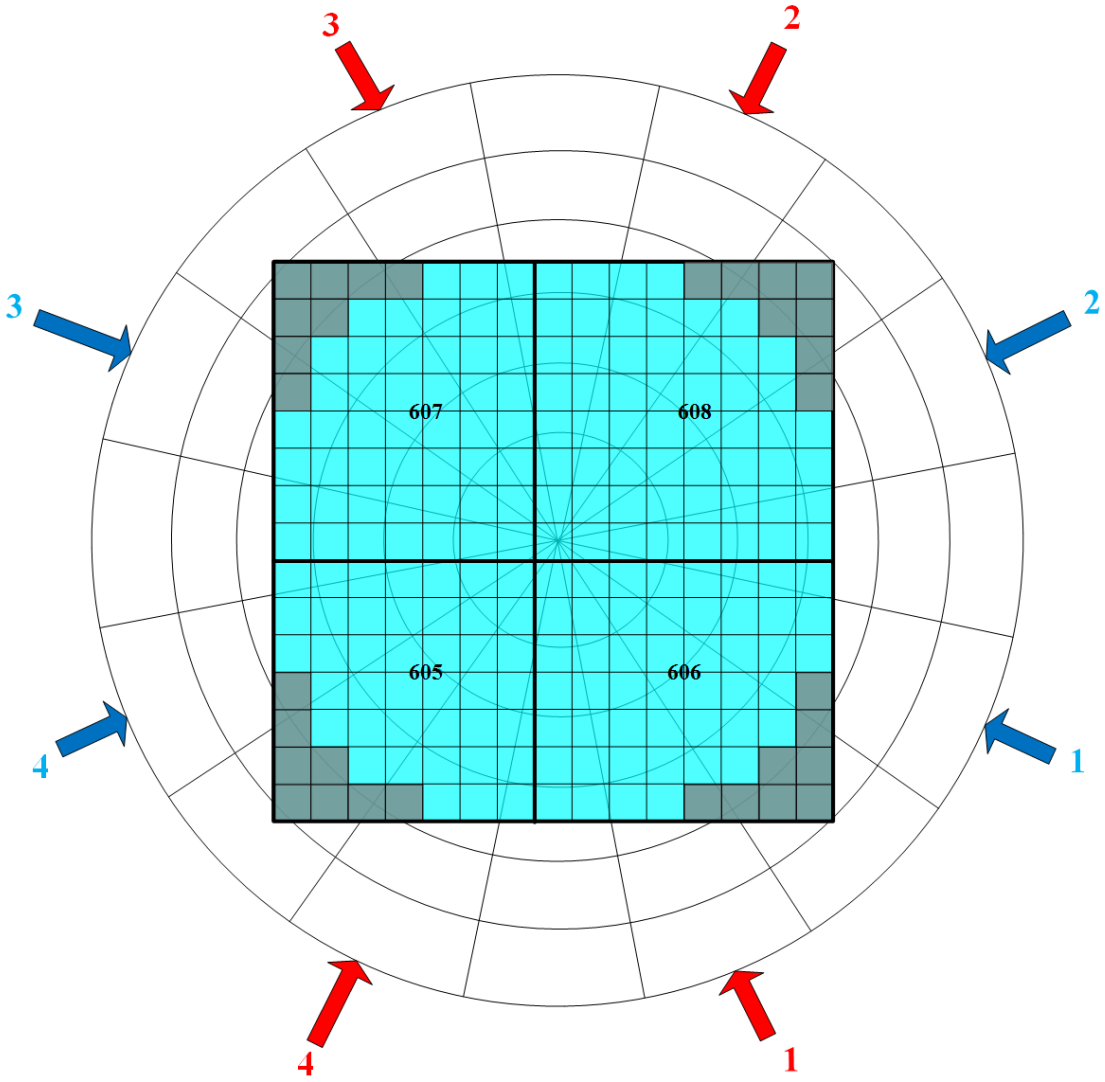

Figure 3.9. Illustration showing an overlay of the Cartesian geometry of the core along with the cylindrical geometry of the plena and the corresponding hot leg (in red) and cold leg (in blue) junctions after a rotation of cylindrical components by 11.25°.

				587.5	593.2	594.2	593.8	594.2	593.2	587.5				
		588.0	601.8	621.5	624.4	625.6	624.9	625.6	624.4	621.5	601.7	587.9		
	588.1	620.0	625.0	624.8	621.3	625.1	617.6	625.1	621.2	624.8	625.0	620.1	588.0	
	600.4	624.7	619.9	617.3	625.8	619.1	615.1	619.1	625.9	617.2	619.9	624.8	600.4	
588.7	621.6	624.7	617.0	623.4	617.4	625.8	619.6	625.8	617.3	623.5	616.9	624.7	621.7	588.5
593.7	624.4	621.2	625.7	617.2	624.2	617.7	624.7	617.7	624.3	617.1	625.8	621.2	624.4	593.6
594.7	625.5	624.9	618.6	625.6	617.7	625.8	619.7	625.8	617.6	625.6	618.5	624.9	625.6	594.5
594.1	624.6	617.1	614.9	619.7	624.6	619.6	614.8	619.7	624.6	619.6	614.9	617.3	624.7	594.0
594.6	625.5	624.9	618.6	625.6	617.6	625.8	619.6	625.9	617.6	625.6	618.7	624.9	625.5	594.6
593.7	624.4	621.2	625.7	617.1	624.3	617.6	624.7	617.5	624.4	617.1	625.8	621.2	624.4	587.5
588.6	621.6	624.7	616.9	623.5	617.2	625.9	619.6	625.8	617.1	623.6	616.9	624.8	621.3	588.9
	600.4	624.7	619.9	617.2	625.9	619.0	615.0	619.0	625.8	617.3	620.0	624.8	600.4	
	588.1	620.0	625.0	624.8	621.2	625.1	617.6	624.9	621.2	624.8	625.1	620.4	588.4	
		587.9	601.7	621.5	624.4	625.5	624.8	625.5	624.4	621.8	601.2	587.8		
				587.5	593.2	594.2	593.9	594.3	593.3	587.5				

Figure 3.10. Illustration showing the peak cladding temperature in Kelvin for all 193 fuel assemblies when the cylindrical components are not rotated.

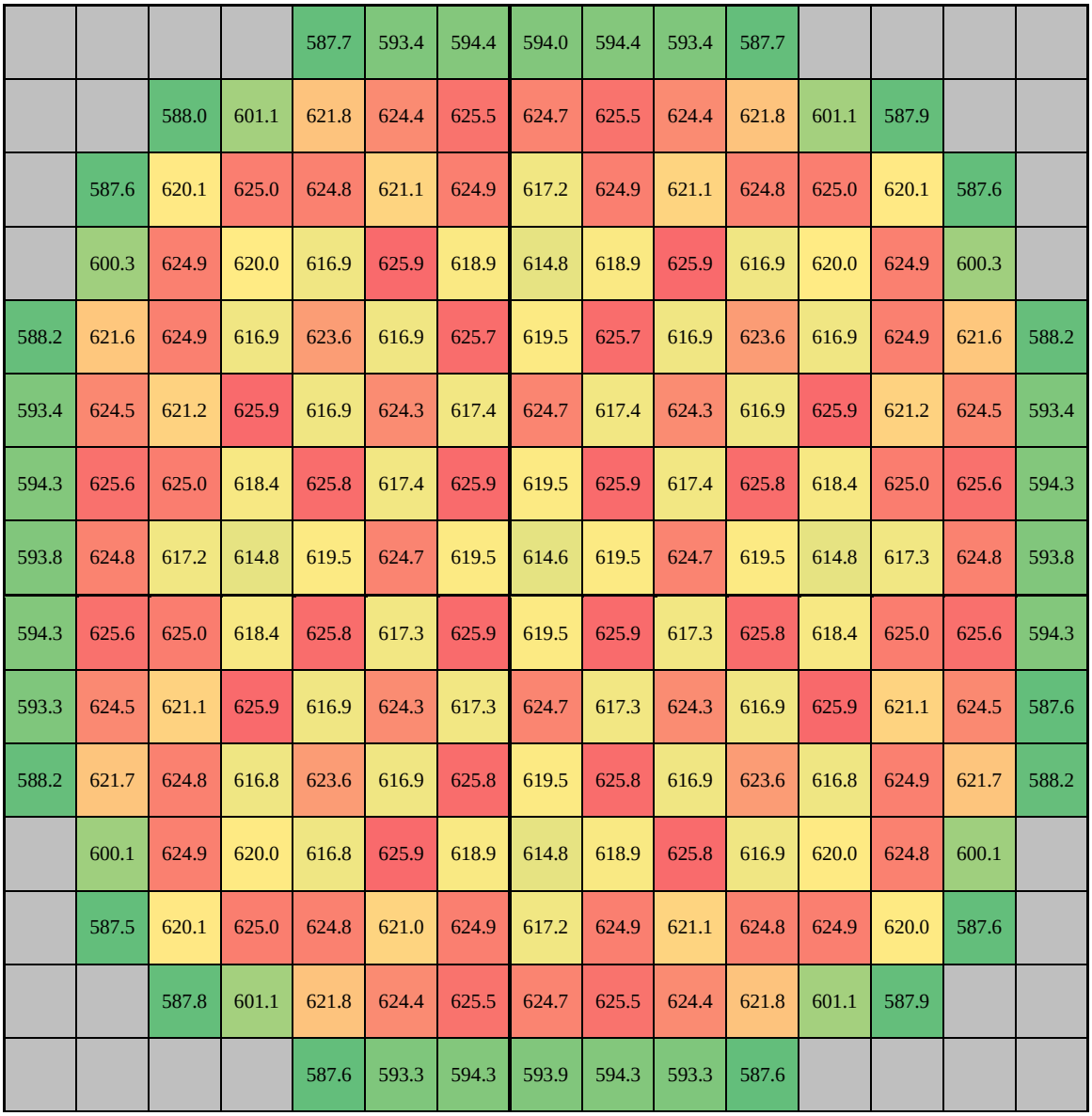

Figure 3.11. Illustration showing the peak cladding temperature in Kelvin for all 193 fuel assemblies when the cylindrical components are rotated.

Table 3.4. Values for pressure and mass flow for four symmetric fuel channels with and without rotated cylindrical components.

		Without Rotation				**With Rotation**			
	Fuel Channel ID	Core Exit	Core Entry	Difference	Absolute Deviation from the Mean Difference	Core Exit	Core Entry	Difference	Absolute Deviation from the Mean Difference
Pressure (psia)	608606	2264.60	2272.65	-8.047	-0.01	2264.13	2272.15	-8.018	0.00
	607306	2264.60	2272.65	-8.049	-0.01	2264.13	2272.15	-8.018	0.00
	605303	2264.60	2272.65	-8.047	-0.01	2264.13	2272.15	-8.013	0.00
	606603	2264.65	2272.65	-7.992	0.04	2264.14	2272.15	-8.010	0.00
Mass Flow (lb/min)	608606	187.28	184.42	2.866	1.08	185.32	184.84	0.478	0.21
	607306	187.35	184.42	2.930	1.14	185.32	184.84	0.481	0.21
	605303	187.19	184.42	2.768	0.98	184.98	184.85	0.129	-0.14
	606603	183.01	184.42	-1.404	-3.19	184.83	184.85	-0.015	-0.28

3.5. Improvements in the Soundness of the Model

After the geometry of the model had been improved to better represent typical PWRs, the results of the steady-state simulation were analyzed for abnormalities. Examples of abnormalities that were encountered included oscillations in flow, pressure, or temperature; excess vaporization of the primary coolant; and asymmetry in the results

(e.g. differing mass flow in the four cold legs). Several causes for these abnormalities were proposed. In order to test each hypothesis, the model was simplified to decrease computational time and decrease the number of possible sources of error. As part of this process, several new models were created. These models consisted of a three-dimensional core with one-dimensional analogues for all other components. From the results of these models, modifications were made to the RELAP5-3D input deck.

In order to prevent non-physical oscillations, a number of changes were added to the original input deck. The first set of changes involved changing the power distribution of the core by modifying the multiplier values defined for each of the 193 heat structures of the core region. The original three-dimensional model used the same axial power profile that was used in the one-dimensional reference model. The power in each of the heat structures was taken to be $\frac{1}{193}$ of the total power used in the heat structures of the one-dimensional model. Thus, the overall power of the core was the same. However, it was determined that this technique led to oscillations in several parameters, including control volume pressure and junction flow rates with respect to simulation time. The solution to this problem was to create a laterally varying distribution of power in the core. The chosen power distribution was based on the consideration of PWR data. Figure 3.12 compares the total primary system flow rate of the laterally uniform core with that of the laterally varying core. In this plot, the ordinate indicates the deviation of the total primary system flow rate to the mean value of the total primary system flow rate. This plot helps illustrate the magnitude of the

oscillations that were present when uniform heat structures were used. While these oscillations were less than 1% of the total flow rate, they were between 400 and 20,000 times larger than the oscillations present when laterally varying heat structures were incorporated.

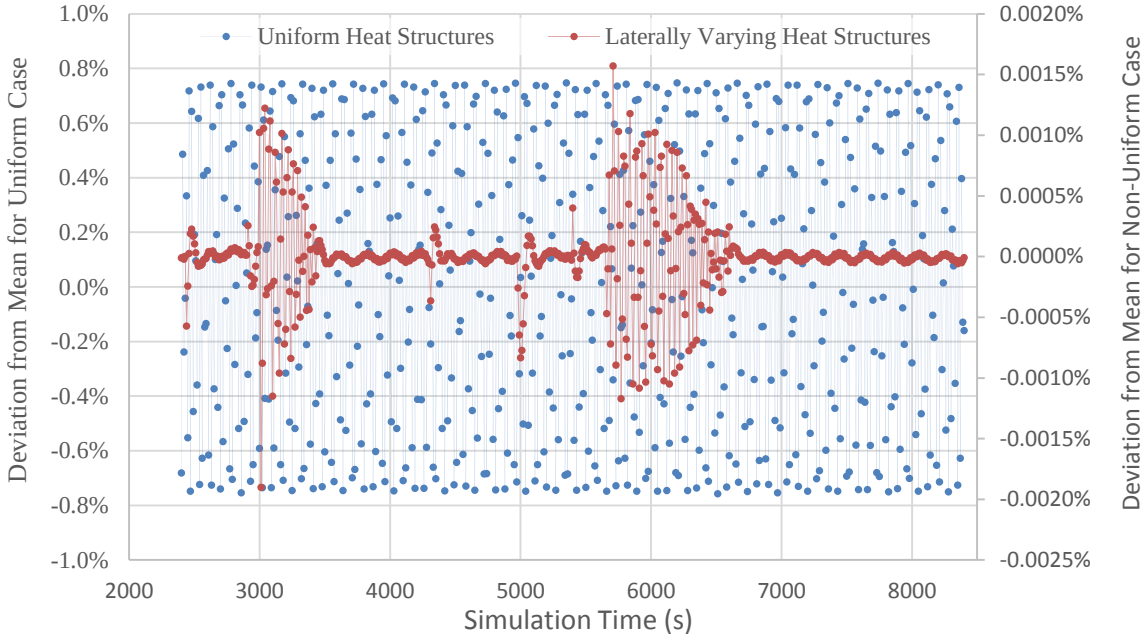

Figure 3.12. Comparison of the changes in the primary mass flow rate for uniform and non-uniform heat structures with respect to simulation time.

Another source of oscillations was determined to be the core bypass nodalization. The core bypass was modeled as using a one-dimensional pipe component (551) and a one-dimensional branch component (550). The branch component was connected to the top face of the seventh (of eight) radial ring of the lower plenum (535).

The inlet of the pipe was then taken to be the outlet of the branch component. Lastly, the pipe component had an outlet to the bottom face of the fifth (of six) radial ring of the vessel exit region (865). In order to most closely model the bypass flow, sixteen junctions were used for both the entry and exit of the core bypass. Each of these junctions was connected from the one dimensional control volume to a unique control volume in the specified three-dimensional ring (corresponding to each of the 16 angular wedges used in the cylindrical components). Such an arrangement was chosen to integrate this one-dimensional component with three-dimensional components, while preserving the flow information being produced in the three-dimensional nodalization. This design choice could be modified if the intended applications of this model were to change. For example, if a spatially dependent flow path was created between the core bypass and the reactor core (e.g. if pressure relief holes were added to the model), then a three-dimensional nodalization of the core bypass may be necessary to correctly simulate the associated phenomena during a transient.

The total flow area in the junctions between the core bypass and the neighboring volumes was preserved from the one-dimensional model such that each junction had only $1/16^{th}$ of the flow area of the one-dimensional analogue. Since the junction in the one-dimensional model already had a relatively small flow area, the flow areas of the junctions in the three-dimensional model were especially minute. In the original three-dimensional model, the junction flag that activates the abrupt area change functionality between the core bypass and its neighboring volumes was preserved. Normally, this

junction flag enables RELAP5-3D to calculate some unique flow characteristics that occur when a flow path is subjected to a junction that has an abrupt change in flow area. However, it was determined that this functionality was no longer compatible with the chosen nodalization, thus changes had to be implemented in the three-dimensional model. The resulting model sets the junction flag that deactivates the abrupt area change functionality for these specified junctions. Figure 3.13 illustrates the total primary flow rate with these flags turned on and off to help express the types of oscillations that were resolved by implementing these changes.

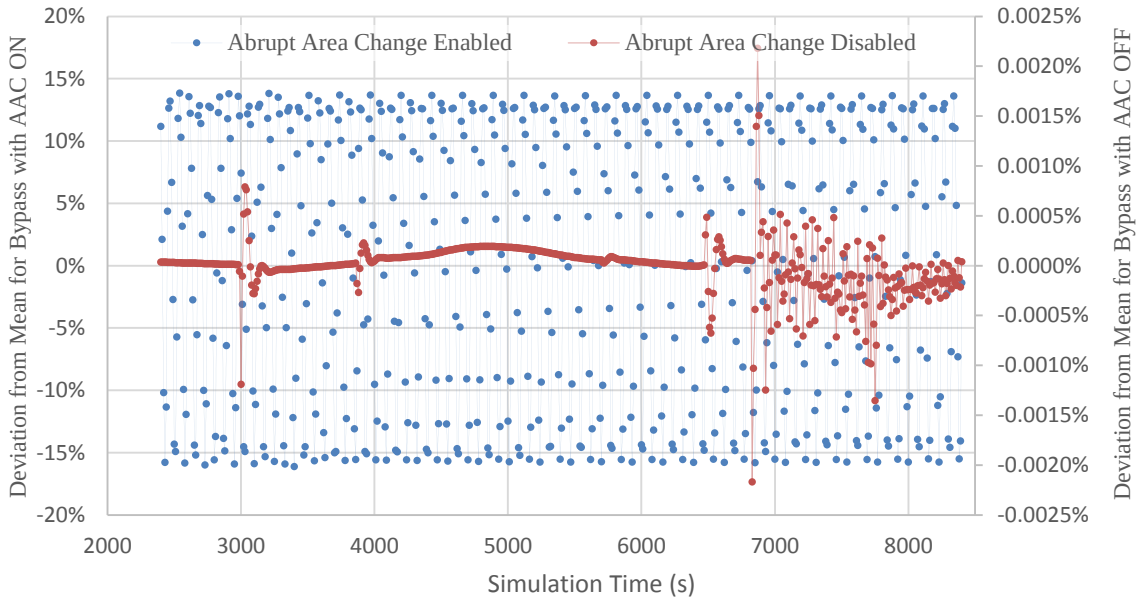

Figure 3.13. Comparison of the changes in the primary mass flow rate with respect to simulation time for cases with the abrupt area change model enabled and disabled.

Lastly, it was determined that fuel temperatures of certain nodes of heat structures with large thermal powers were much higher than anticipated. It was hypothesized that some nodes may have been experiencing departure from nucleate boiling during the steady-state calculation. Such an event would result in a change of heat transfer mechanisms from nucleate boiling to film boiling. This hypothesis was confirmed by the request of the "htmode" control variable that provides the heat transfer regime for a surface. This variable request showed that the heat transfer mode changed from subcooled nucleate boiling to subcooled film boiling with subcooled transition boiling being an intermediary of the two lasting for less than two seconds. During the same period, the heat transfer coefficient at the boundary dropped by a factor of 40, and failed to recover.

The root cause of this error was determined to be an error in the input deck. While a heat structure connected to a one-dimensional hydrodynamic volume has a straightforward mechanism to determine heat transfer from the structure to the volume, three-dimensional nodalizations are more complex. RELAP5-3D does not calculate wall heat transfer correlations by using correlations for three-dimensional flow, but instead relies on a single coordinate direction (RELAP5-3D Manuals, 2012). This coordinate direction for one-dimensional control volumes is obvious due to the fact that only one-dimension is simulated in the problem, however, for three-dimensional control volumes this must be defined by the user. The initial three-dimensional model used the x-coordinate (lateral coordinate), which resulted in departure from nucleate boiling. When

the model was corrected to use the z-coordinate (axial coordinate), all nodes of all heat structures were well below the critical heat flux, at which departure from nucleate boiling occurs. Figures 3.14 and 3.15 illustrate the RELAP5-3D simulated values for heat flux, critical heat flux, and fuel cladding temperature for a "hot node," with the x-coordinate and the z-coordinate selected for heat transfer correlations, respectively. In Fig. 3.14, departure from nucleate boiling occurs at 40 seconds.

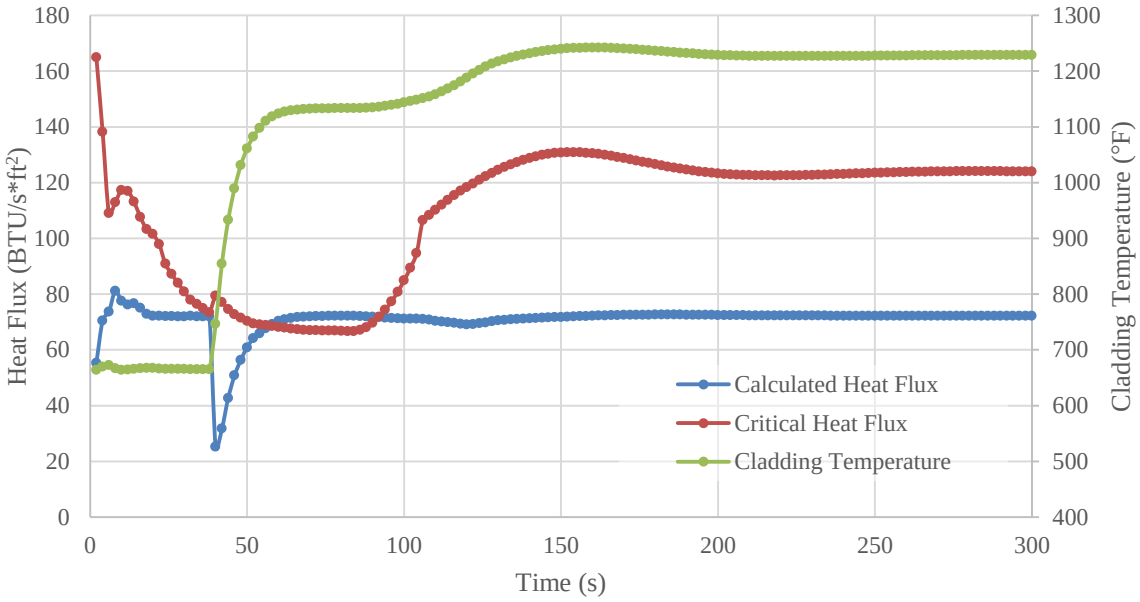

Figure 3.14. Local heat flux, critical heat flux, and fuel cladding surface temperature for a "hot node" with the x-coordinate used for heat transfer correlations.

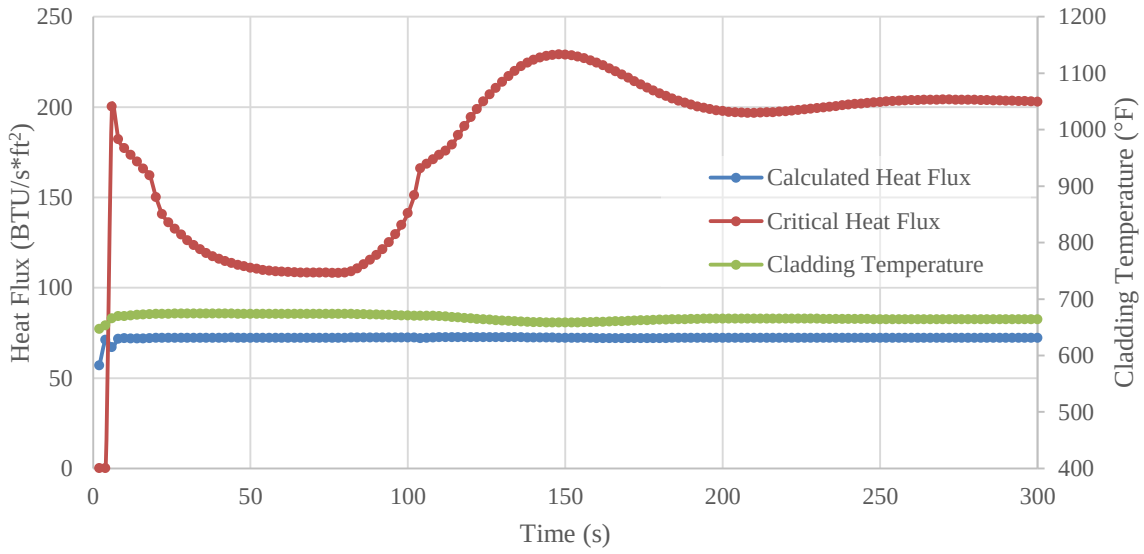

Figure 3.15. Local heat flux, critical heat flux, and fuel cladding surface temperature for a "hot node" with the z-coordinate used for heat transfer correlations.

3.6. Model Finalization

After the anomalies discussed above were eliminated, the resulting nodalization was used as a framework for further development. The next phase of the project sought to make the 3D model into better agreement with the 1D reference model. In order to do this, the 3D model was run with many intermediate steps, with each intermediate step being placed into agreement with the 1D reference.

In practice, this meant that a largely 1D model was run where the only 3D component was the vessel entry region. By comparing the results of the new model with

those of the 1D reference, new values for nodal form pressure losses ("k-loss values") and model flags were hypothesized. These new values were then used to build a new model. This process was repeated until the intermediate model was found to be in good agreement with the 1D model. Next, the 3D downcomer nodalization was added to the existing model. After this new nodalization was found to be in agreement, the process was continued in the same systematic fashion until all 3D components had been added to the model and found to be in good agreement with the 1D reference values at each stage of the process.

4. MULTIPLE JUNCTION TOOL

As part of this thesis work, a tool was developed for use in conjunction with the RELAP5-3D program. This tool was written in the FORTRAN, and compiled and executed on a UNIX machine. In order to execute this tool, an input deck is required. The requirements and format of this input deck are described in the tool input section of this thesis.

4.1. Description of the Problem

After review of the modeling approach section, it is apparent that the nodalization of the model changes several times during its development. These changes help establish parametric sensitivities to the nodalization, as well as the underlying equations that the RELAP5-3D code eventually solves. However, creating new nodalizations using three-dimensional components can be arduous.

Two of the most difficult places to implement a three dimensional model are the interfaces between the plena and core plates due to their geometry. Both the lower and upper plena are modeled as cylindrical components with mesh spacing defined in terms of an incremental radial distance (Δr), an incremental angular distance ($\Delta \theta$), and an incremental height (Δz). By contrast, both the lower and upper core plates use rectangular geometry, consisting of a mesh defined by an incremental width (Δx), an

incremental depth (Δy), and an incremental height (Δz). RELAP5-3D does not have the capability to solve for the "overlaying" or "adjoining" areas between nodes. Instead, RELAP5-3D uses by default the smaller area of any two connecting areas as the flow area (RELAP5-3D Manuals, 2012). In order to use this default, each node would only be able to have a single junction at the interface, and neither the flow area nor the flow path would be correctly modeled. Thus, when designing the input deck, the adjoining area must be calculated by the user.

This task is tedious and may introduce errors into the input deck. In the three-dimensional reference model, the flow area between any two nodes was estimated to the nearest one-fifth of the smaller nodal volume (representing one of 193 active flow channels in the core plate). For the initial PWR model discussed in this thesis, the resolution was increased to account for areas as small as one-eighth of a core plate node. In order to estimate these areas, the interfacial geometry was plotted using Microsoft Excel. Since the interface between a core plate and a plenum is symmetric in an octant, the estimation was performed for only one octant, as shown in Fig. 4.1. In this figure, each value represents the flow area between the adjoining nodes divided by the total flow area of a single core plate (rectangular) node. After establishing the flow area for a single octant, a relationship table was created for the different nodes of the core plate.

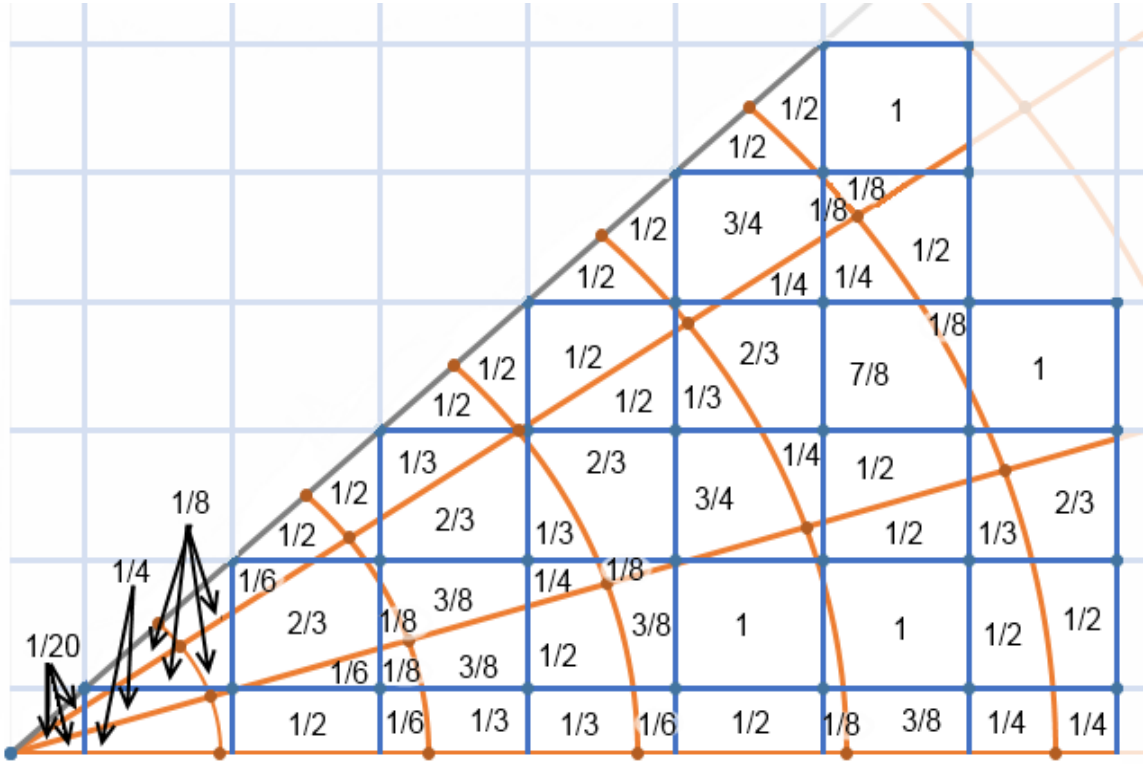

Figure 4.1. Illustration depicting the estimation of the adjoining area at the core plate-plenum interface.

While the core plate consists of 193 active nodes, the simplest way to model the plate is by using 225 nodes in a 15 by 15 arrangement and "removing" the 32 excess nodes. Additionally, RELAP5-3D only allows a component to have 99 nodes. Thus, the core plates must be modeled using at least 3 components. In both the three dimensional reference model and the model presented in this thesis, the core and both core plates are modeled by the combination of a 7 by 7 component, a 7 by 8 component, an 8 by 7

component, and an 8 by 8 component. The nodalization of the core is shown in Fig.4.2. The RELAP5-3D node number is provided in the upper box of each cell (of the form CCCXYY, where CCC is the component number, X is the x position number, and YY is the y position number), while the symmetry number is provided in the lower box of each cell. By using octant symmetry, only 31 nodes must be analyzed. The symmetry number is used to relate different nodes that will have the same interfacial geometry and adjoining areas. The excess nodes feature gray boxes instead of symmetry numbers. These cells are removed from the simulation and are not used in the calculation of adjoining areas. This nodalization is identical to that of the lower and upper core plates, with the exception of the first two nodal digits. For the lower core plate, "60CXYY" is replaced by "54CXYY," while the upper core plate uses nodes with the form "84CXYY."

607108	607208	607308	607408	607508	607608	607708	608108	608208	608308	608408	608508	608608	608708	608808
				31	30	29	28	29	30	31				
607107	607207	607307	607407	607507	607607	607707	608107	608207	608307	608407	608507	608607	608707	608807
		27	26	25	24	23	22	23	24	25	26	27		
607106	607206	607306	607406	607506	607606	607706	608106	608206	608306	608406	608506	608606	608706	608806
	27	21	20	19	18	17	16	17	18	19	20	21	27	
607105	607205	607305	607405	607505	607605	607705	608105	608205	608305	608405	608505	608605	608705	608805
	26	20	15	14	13	12	11	12	13	14	15	20	26	
607104	607204	607304	607404	607504	607604	607704	608104	608204	608304	608404	608504	608604	608704	608804
31	25	19	14	10	9	8	7	8	9	10	14	19	25	31
607103	607203	607303	607403	607503	607603	607703	608103	608203	608303	608403	608503	608603	608703	608803
30	24	18	13	9	6	5	4	5	6	9	13	18	24	30
607102	607202	607302	607402	607502	607602	607702	608102	608202	608302	608402	608502	608602	608702	608802
29	23	17	12	8	5	3	2	3	5	8	12	17	23	29
607101	607201	607301	607401	607501	607601	607701	608101	608201	608301	608401	608501	608601	608701	608801
28	22	16	11	7	4	2	1	2	4	7	11	16	22	28
605107	605207	605307	605407	605507	605607	605707	606107	606207	606307	606407	606507	606607	606707	606807
29	23	17	12	8	5	3	2	3	5	8	12	17	23	29
605106	605206	605306	605406	605506	605606	605706	606106	606206	606306	606406	606506	606606	606706	606806
30	24	18	13	9	6	5	4	5	6	9	13	18	24	30
605105	605205	605305	605405	605505	605605	605705	606105	606205	606305	606405	606505	606605	606705	606805
31	25	19	14	10	9	8	7	8	9	10	14	19	25	31
605104	605204	605304	605404	605504	605604	605704	606104	606204	606304	606404	606504	606604	606704	606804
	26	20	15	14	13	12	11	12	13	14	15	20	26	
605103	605203	605303	605403	605503	605603	605703	606103	606203	606303	606403	606503	606603	606703	606803
	27	21	20	19	18	17	16	17	18	19	20	21	27	
605102	605202	605302	605402	605502	605602	605702	606102	606202	606302	606402	606502	606602	606702	606802
		27	26	25	24	23	22	23	24	25	26	27		
605101	605201	605301	605401	605501	605601	605701	606101	606201	606301	606401	606501	606601	606701	606801
				31	30	29	28	29	30	31				

Figure 4.2. Nodalization of the core in RELAP5-3D, with symmetrical channels labeled.

Not only is this process time-consuming, it may introduce human error into the input deck, which could propagate into other errors after RELAP5-3D execution. The propagation of any possible errors is complex, and requires a sophisticated analysis of the output sensitivity to the input parameters affected by this method. As a solution to this problem, the tool presented in this thesis is capable of determining the adjoining flow area between any components that share an interface. This tool reads in the spatial

component data and overall initial conditions from a user-supplied input deck, and outputs the corresponding junction card that contains information on the adjoining areas as well as the initial liquid and vapor flow rates through each junction.

4.2. Tool Input

The input for the tool is provided as a text file with the file name “usrinp.inp”. This file contains information that dictates the problem geometry to the tool and how the user wants the tool to evaluate the geometry. The actual input consists of up to 5 main sections: 1) user options, 2) geometry start point initializations, 3) full geometry declarations, 4) geometry exclusion options, and 5) geometry symmetry options. These sections are summarized in Table 4.1.

Table 4.1. Card numbers and descriptions for the input deck of the multiple junction tool.

Card Number	**Card Description**
1-1	Area calculation method. Enter '1' for the 'deterministic' scheme, '2' for the 'random' scheme, or '3' for the 'orthogonal' scheme.
1-2	The component number for the first multiple junction card. If more than one card is needed, they will be sequentially numbered.
1-3	The maximum number of junctions per card. If symmetry options are used, the maximum number of junctions should be divisible by the number of symmetrical components (i.e. 2 for half, 4 for quarter, 8 for octant).
1-4	The resolution of the problem. This number controls the mesh spacing used in the numerical scheme. The larger the resolution, the smaller the mesh spacing becomes. It is suggested to use values between 100 and 500.

Table 4.1. Continued.

Card Number(s)	Card Description
1-5	The initial flow rates for the total area. These are identical to the flow rates used by RELAP for the initial liquid and vapor flow rates.
1-6	Forward and backward loss coefficients.
2-1	From geometry. This card uses the flag 'from' followed by the number of components in the 'from' direction.
2-2…n	These are the card numbers and initial points in space (x,y,z) or (r,θ,z) for each component in the 'from' direction, with each component having its own line.
3-1	To geometry. This card uses the flag 'to' followed by the number of components in the 'to' direction.
3-2…n	These are the card numbers and initial points in space (x,y,z) or (r,θ,z) for each component in the 'to' direction, with each component having its own line.
4-1	The keyword 'start' is used to separate this section.
4-2,3,4,5… n*4+1,n*4+2, n*4+3,n*4+4	These cards are the RELAP cards CCC0001 and CCC0XNN. For more information, please refer to Appendix A of RELAP Manual 2.
5-1	The keyword 'exclude' is used to begin the exclusion options section.
5-2…n	Each line has a unique node number that will be excluded from the area calculation. One use for these numbers is to not calculate area that is adjoined to a node which was initialized but contains no flow.
6-1	The keyword 'symmetry' is used to begin the symmetry section
6-2	The type of symmetry for the problem (i.e. 'half', 'quarter', or 'octant)
6-3	The first domain indicator (e.g. x>0.0000000)
6-4	The second domain indicator (e.g. y>0.0000000)
6-5…n	Symmetry Definitions. Each line consists of a node and the corresponding nodes that share its symmetry. The number of nodes must be consistent with the symmetry option selected (e.g. if 'quarter' is selected, then each line should contain 4 numbers.)
7-1	The keyword 'end' signals the end of the input deck.

4.3. Tool Implementation

The primary function of the tool is to calculate the adjoining area between RELAP5-3D components. In order to fulfill this function, several secondary functions are included such as input reading, the exclusion of nodes from the calculation, forced symmetry, and output writing. These secondary functions help to facilitate the primary functionality and add user control to the problem. First, the implementation of the tool primary functionality is discussed.

Three methods for area calculation are incorporated into the multiple junction tool. These methods are a "deterministic /systematic" method, a "random/Monte Carlo" method, and an "orthogonal/Latin Hypercube Sampling (LHS)" method. Figure 4.3 provides an illustration of these three methods, which will also be described in detail in this text. A fourth "integral" method was also proposed, but it has not yet been implemented due to the difficulty to generalize such a method, the computational costs, and the relative strength of the other methods discussed here.

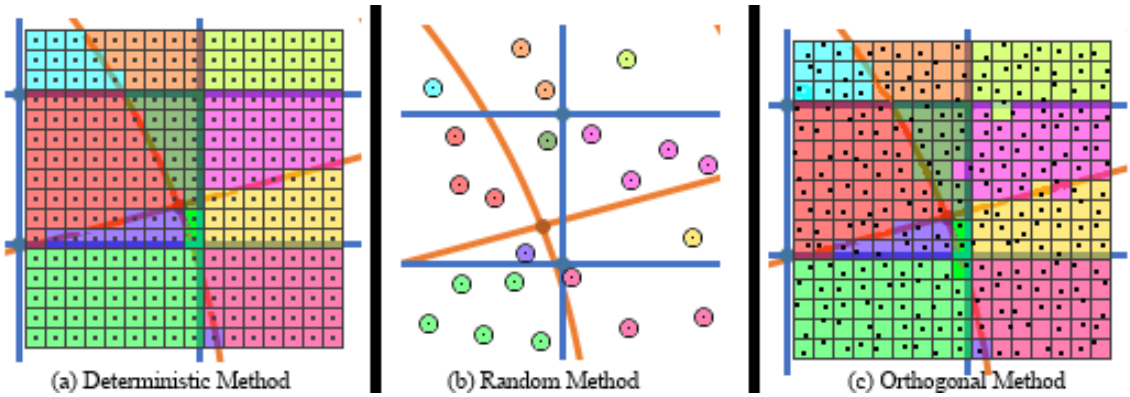

Figure 4.3. Illustration of the three methods used for calculation of adjoining areas. An excerpt of Fig. 4.1 is used, with each unique color representing an area or tally that is assigned to a specific nodal pair.

The deterministic method creates a spatial mesh of very small squares. The area of each square is assigned to the centroid of the square. The code then calculates the area between any two adjacent nodes according to the number of centroids that the nodal pair contains. While this method is reasonably accurate, it is predicted that systematic errors may occur as the error associated with representing each square as a centroid may begin to form patterns in the geometry. For example, if centroids are located along the line $y = 0.0001x$, and $y = 0$ is a component edge, then all of the centroids will fall into the component located at $y > 0$, and all of the corresponding area from the mesh squares will be assigned to that component.

The second method is a random method. This method does not create a spatial mesh. Instead, this method generates random points that lie on the surface interface and

tallies the number of points that fall within each possible pair of nodes. These tallies are then normalized to the overall total interfacial area. This method removes the systematic error associated with the deterministic method. However, this method also introduces stochastic error, especially when few sample points are taken.

The third method is an orthogonal method. This method blends the previous two methods together. In order to implement this method, the interfacial area is broken up into a grid of small squares, similar to the deterministic method. However, instead of assigning the area of each square to the centroid, a random point within each is square is chosen. This point then carries the weight of the entire square's area with it as it is assigned to a nodal pair. The orthogonal method results in a reduction of the overall error in comparison to the deterministic and random methods.

In addition to calculating the adjoining area, the tool has other capabilities that add robustness. One feature of the tool is the ability to exclude certain nodes from the area calculation. While each core plate consists of 225 nodes, flow is only permitted through 193 of these. The tool is capable of excluding the 32 unused nodes from the calculation of adjoining areas.

Another feature of the code is to force symmetry. Since both the random and orthogonal area calculation methods rely on random numbers, the results will intrinsically not be perfectly symmetrical even if the physical model is assumed to be so. In order to account for this, the user is able to specify a problem domain for the tool to consider in the adjoining area calculations. The code is then capable of extrapolating the

results from the specified domain to other regions that are geometrically identical, provided the user has requested such a method on the input deck.

4.4. Tool Output

The output from the tool is designed to be as user friendly as possible. The output is provided in a text file named "mjout.out". This text file has several "echoes" of the user's input, including a table listing components as 'to' or 'from' with their respective component numbers and initial positions.

The output also provides a table that describes all of the nodes created based on the RELAP5-3D input information, including bounds for the primary (x or r), secondary (y or θ), and tertiary (z) axis values of each node. Following the "echo" section of the output file, the problem domain is stated, as well as the total calculated area of all the nodal pairs summed together. In order to increase functionality with the RELAP5-3D program, a cutoff area has been implemented into the tool. Volumes that are connected by an area less than the cutoff are excluded from the consideration. However, the output file provides areas with the cutoff and without the cutoff. This enables the user to confirm that the results are acceptable when using a cutoff.

Lastly, multiple junction cards are provided in the output file. These cards have the correct format for use with the RELAP5-3D code. This enables easy implementation

into an existing input deck, and quick modification when a model's nodalization is changed.

4.5. Tool Verification and Validation

According to the Institute of Electrical and Electronics Engineers (IEEE) Standard Computer Dictionary, verification is, "The process of evaluating a system or component to determine whether the products of a given development phase satisfy the conditions imposed at the start of that phase (Standards Coordination Committee of the IEEE Computer Society, 1990)." Put simply, verification can be thought of as "building the product right" or "solving the equations correctly." Conversely, the IEEE definition for validation is, "The process of evaluating a system or component during or at the end of the development process to determine whether it satisfies specified requirements." Validation can also be thought of as "building the right product" or "solving the correct equations."

For the multiple junction tool, both verification and validation were performed. Verification consists of ensuring that the tool successfully approximates the exact area from certain samples of the adjoining areas. Validation consists of ensuring final RELAP5-3D results that are precise and accurate.

4.5.1. Tool Verification

The tool was verified by comparing tool-calculated area adjoining two nodes with the exact area calculated manually. Two examples of this effort are provided in this thesis.

First, consider the central fuel channel of the reactor. This channel forms an interface with the center of the cylindrical components, as shown in Fig. 4.4, where the blue lines correspond the boundaries of the Cartesian control volume representing the central channel of the core plate, while the orange lines correspond to the boundaries of the cylindrical nodes representing the plena. Since the cylindrical component consists of 16 angles of 22.5° each, and the Cartesian component is a perfect square, only two unique triangles are formed, labeled '#1' and '#2' in the figure. If w is the mesh spacing of the Cartesian component (i.e. the length of one side of the blue square), then the areas of triangle #1 and triangle #2 and be calculated using Eqs. 4.1 and 4.2, respectively.

$$A_1 = \frac{1}{8} * w^2 * \tan(22.5°) \tag{4.1}$$

$$A_2 = \frac{1}{8} * w^2 * [\tan(45°) - \tan(22.5°)] \tag{4.2}$$

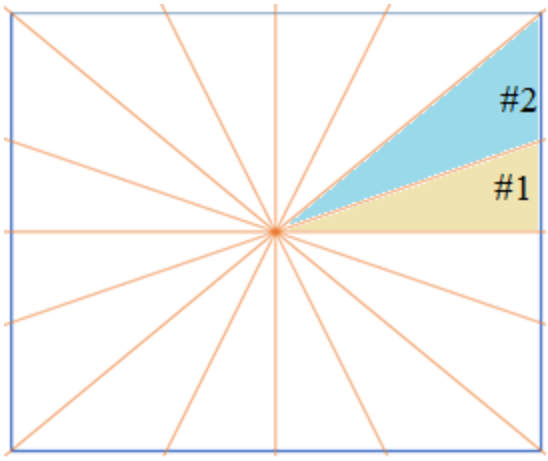

Figure 4.4. Illustration of the interface between the central core plate channel and the center of a cylindrical plenum component.

These arithmetically calculated values can be compared to the values calculated by the multiple junction tool to verify that the tool is working as intended. Figures 4.5 and 4.6 illustrate the areas of triangles #1 and #2, respectively, as calculated by the tool as a deviation from the actual arithmetic value. These figures also verify all three proposed methods for area calculation: deterministic, random, and orthogonal. While all three methods have been verified, this data most strongly supports using the orthogonal method. The abscissa indicates the resolution value used on the tool input deck. As the resolution increases, the mesh spacing (for the deterministic and orthogonal methods) decreases or the number of "histories" (for the random method) increases. However, as resolution increases, the time required for the tool to execute also increases, as shown by Fig. 4.7.

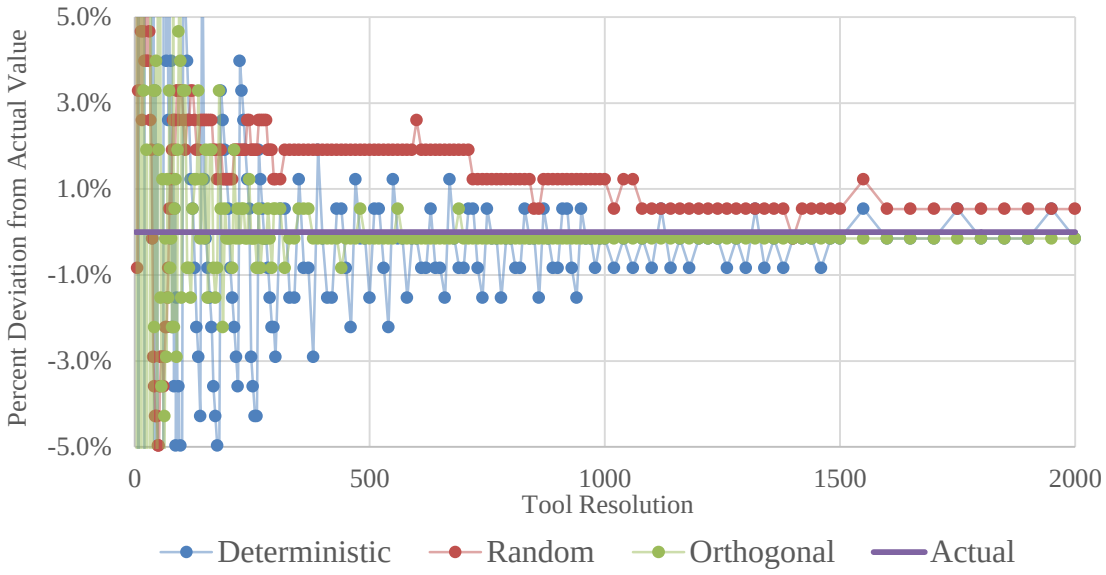

Figure 4.5. Tool verification using triangle #1 of Fig. 4.4 as a reference.

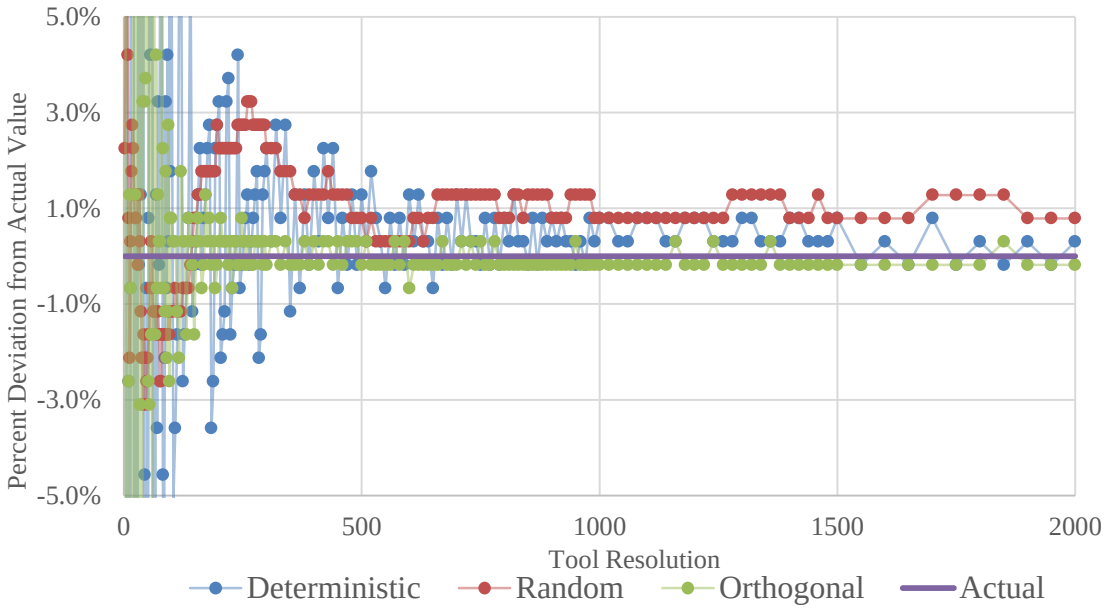

Figure 4.6. Tool verification using triangle #2 of Fig. 4.4 as a reference.

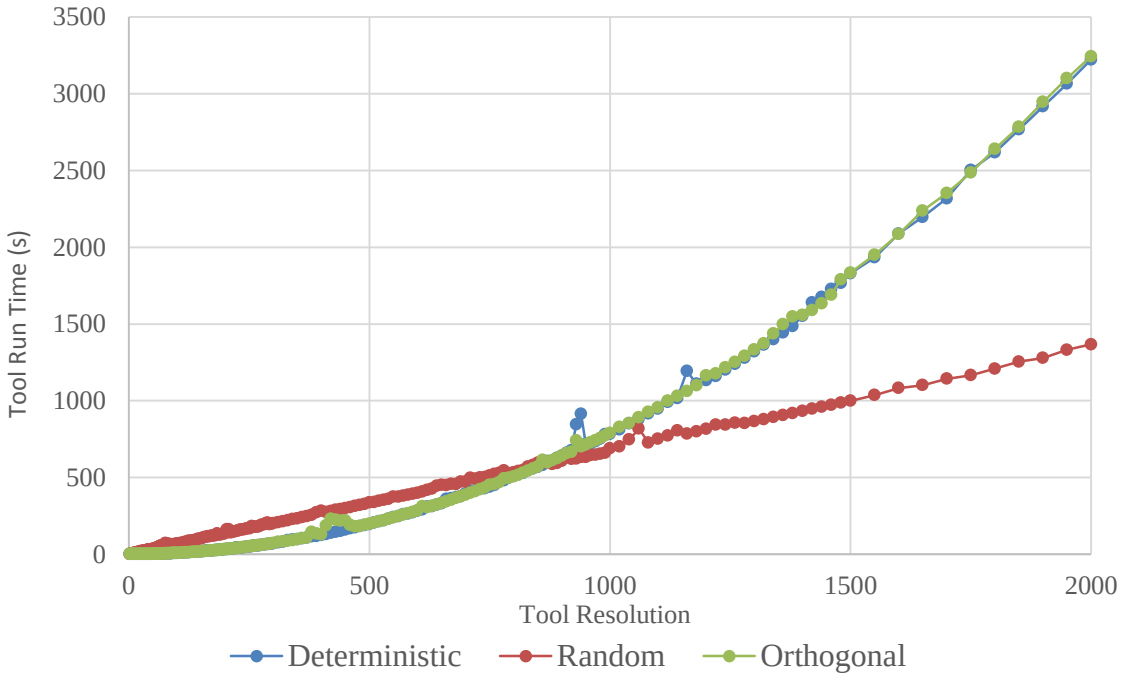

Figure 4.7. Computer run time for each method as a function of tool resolution. Note that anomalies in this data may be caused by other processes on the computer.

A more complicated geometry used in verification is provided as Figure 4.8. Again, the blue lines represent the boundaries of a Cartesian control volume while the orange lines represent the boundaries of a cylindrical control volume. This geometry consists of a single Cartesian flow channel that shares an interface with nodes of belonging to the same angular sector but different radial sectors. The area given by regions #1 and #2 can be calculated using Eqs. 4.3 and 4.4, respectively.

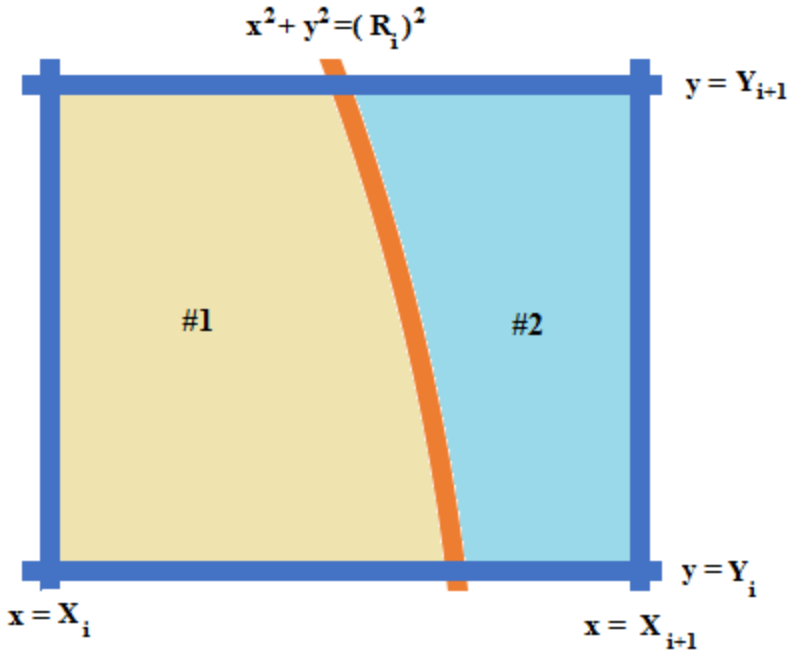

Figure 4.8. Illustration of the interface between a Cartesian node and two cylindrical nodes in the same angular sector.

$$A_1 = \int_{Y_i}^{Y_{i+1}} \sqrt{R_i^2 - y^2}\, dy - \int_{Y_i}^{Y_{i+1}} X_i\, dy \tag{4.3}$$

$$A_2 = \int_{Y_i}^{Y_{i+1}} X_{i+1}\, dy - \int_{Y_i}^{Y_{i+1}} \sqrt{R_i^2 - y^2}\, dy \tag{4.4}$$

Again, the actual area of the two regions is compared to the area calculated by the tool. This is presented as Fig. 4.9 for region #1 and Fig. 4.10 for region #2.

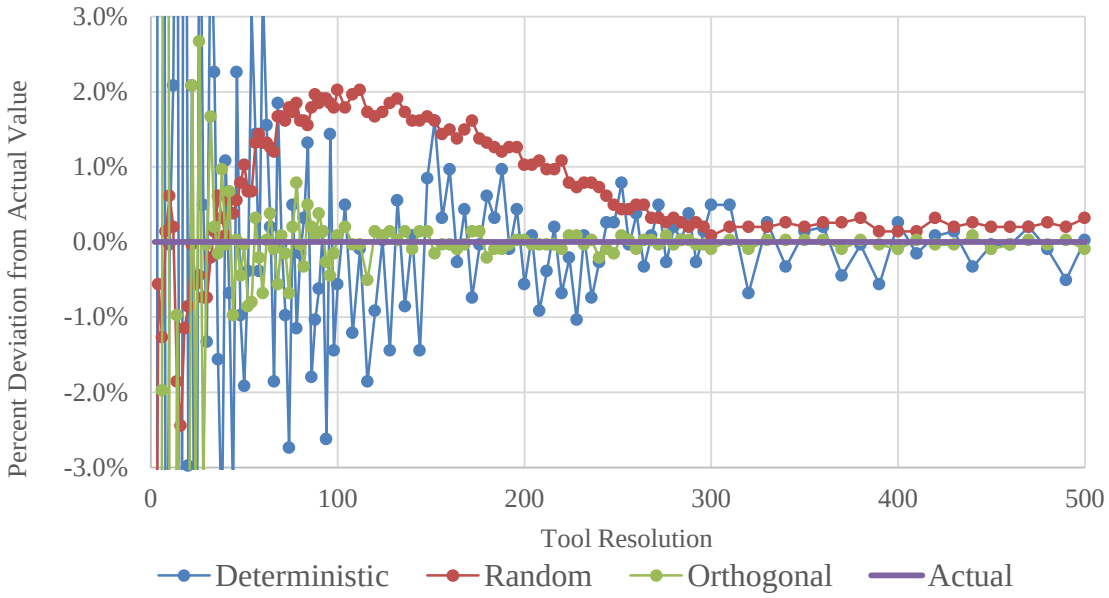

Figure 4.9. Tool verification using region #1 of Fig. 4.8 as a reference.

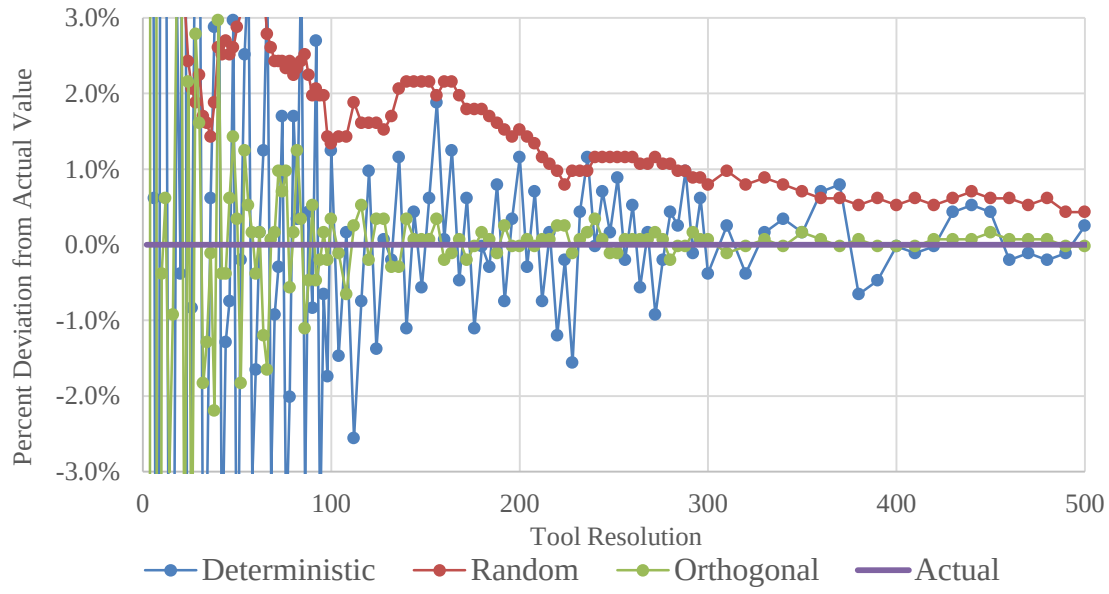

Figure 4.10. Tool verification using region #2 of Fig. 4.8 as a reference.

A comparison of Figs. 4.5 and 4.6 with Figs. 4.9 and 4.10 also conveys an intrinsic property of the tool. In general, the accuracy and precision of the tool calculated areas is better for large adjoining areas than for small adjoining areas. This is because the mesh used in the deterministic and orthogonal methods has a uniform resolution throughout the problem domain, and the random method has no scaling for "importance." Thus, in general, smaller adjoining areas have a larger percent error than larger adjoining areas. Additionally, Figs. 4.5 and 4.6 clearly have discrete calculated values. This is caused by the truncation of the actual area for formatting for RELAP5-3D. In RELAP5-3D, the length of an input line must be 80 characters or less. In order to ensure this criterion is met, flow area is calculated by default to the nearest ten-thousandth (RELAP5-3D allows for area in m^2 or ft^2). While this is considered accurate macroscopically, this also results in a larger percent error when calculating smaller adjoining areas.

One of the features of the multiple junction tool is the use of a cutoff area to discard adjoin areas that are deemed "too small" to influence the correctness of the results. Additionally, having small flow areas for junctions may cause oscillations or errors (RELAP5-3D Manuals, 2012). In fact, volume 5 of the RELAP manuals suggests that "…the modeler should not use a highly reduced junction flow area (e.g., that of the orifice itself). Instead, a junction flow area equal to that of the smaller of the two adjacent volumes should be used along with an increased loss coefficient as needed to limit the flow to the desired value." This phenomenon is also discussed in section

2.3.3.3 of volume 2 of the RELAP manuals. While this feature is beneficial when the tool is used in conjunction with RELAP5-3D, this feature must be verified such that only acceptable levels of area are "discarded." In order to perform this analysis, all three area calculation methods were compared again to true values; however, instead of using just a small region as a reference, the entire problem domain was considered. That is to say, the tool calculated area will be compared to the actual, total adjoining area of four Cartesian components consisting of 193 total active nodes (e.g. representing the flow channels of the upper core plate region) with one cylindrical component consisting of 96 total nodes (e.g. representing the upper plenum). Figure 4.11 illustrates the deviation of the calculated area when no cutoff is used with the actual area value, while Fig. 4.12 illustrates the deviation of the calculated area when the cutoff feature is enabled. These figures illustrate that all three area calculation methods are capable of accurately calculating the total area when no cutoff is present. However, when a cutoff is used, the three methods tend to converge to approximately 0.03% less area than the actual area. This error is considered acceptable, with the tradeoffs of avoiding very small junctions outweighing those of explicitly modeling them in the RELAP5-3D program.

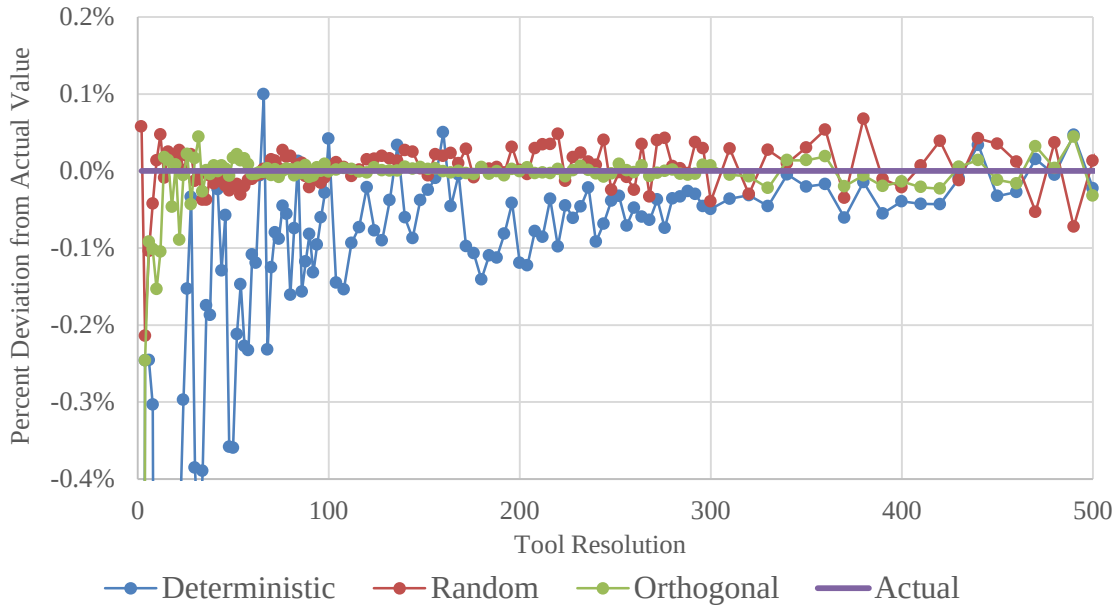

Figure 4.11. Tool verification without a cutoff using the total area as a reference.

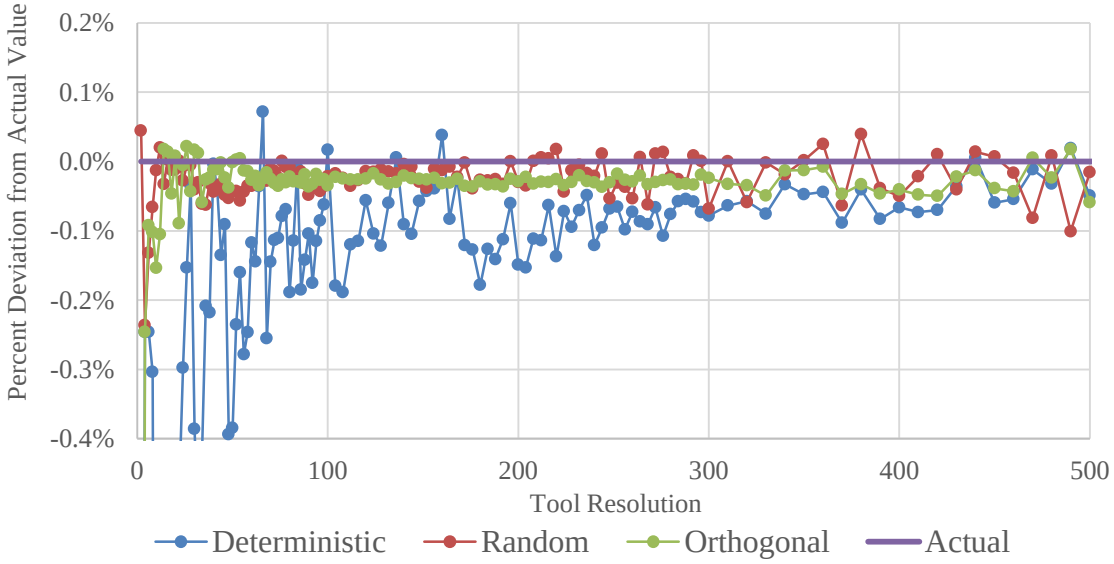

Figure 4.12. Tool verification with a cutoff using the total area as a reference.

By comparing the flow area calculated by the tool with the actual flow area for various regions of the problem, it can be stated with high confidence that the "equations were solved correctly" or that the tool was "built correctly." This holds true for all three area calculation methods, but the orthogonal method converges the most quickly, with a high degree of accuracy and precision. Thus, while all methods and features of the tool have been verified, the best results will likely be produced when the user selects the orthogonal method.

4.5.2. Tool Validation

In order to validate the tool, the tool must be capable of producing results in RELAP5-3D that are as good as or better than results that could be created by attempting to solve the same problem manually. Since the tool has been verified to accurately calculate the flow area between adjoining areas with considerable accuracy and precision, the focus of the tool validation shifts to ensuring the reproducibility of its solutions. The tool has been validated by running the tool twice, once with forced symmetry enabled and once with forced symmetry disabled. The results of the two different methods produced multiple junction cards that are similar to each other, but slightly different. These junction cards were then added to two identical RELAP5-3D input decks (i.e. the only differences in these decks was the multiple junction cards connecting the lower plenum to the lower core plate and the cards connecting the upper

core plate to the upper plenum). These RELAP5-3D cases were then be executed, and the results were compared to check for consistency and similarity. Since the two decks produced similar output, it was determined that RELAP5-3D is insensitive to the effects of the precision of the multiple junction tool. Table 4.2 presents the steady-state values for temperature, mass flow, and pressure in the hot leg entrance node (*00) for all four hot legs and for both RELAP5-3D cases.

Table 4.2. Steady-state parameter values for temperature, mass flow, and pressure in the four RCS hot legs for RELAP5-3D models built using the multiple junction tool with the forced symmetry options both disabled and enabled.

	Hot Leg #	Temperature (°F)	Mass Flow (lb/s)	Pressure (psi)
Symmetry OFF	1	620.75	9680.54	2235.40
	2	620.50	9684.25	2235.46
	3	620.80	9679.55	2235.38
	4	620.40	9682.03	2235.40
Symmetry ON	1	620.62	9683.51	2235.28
	2	620.68	9682.21	2235.25
	3	620.54	9686.96	2235.35
	4	620.38	9687.69	2235.35

These results show that changes in the RELAP5-3D results due to different executions of the multiple junction tool are insignificant in comparison to the accuracy of the rest of the RELAP5-3D model. Even when the reactor vessel is modeled completely symmetrically, consisting of four completely identical “quarters” (identical geometries, flow paths, flow areas, heat structures, etc.) the results have a small

variability between the four legs. This small variability is on a similar order of magnitude as the variability caused by the asymmetrical flow areas calculated by the multiple junction tool when the forced symmetry option is turned off.

5. RESULTS

The steady-state results from the final three-dimensional model must be consistent with the results from the simpler, one-dimensional reference model. During the model development, if there were large disagreements between the one-dimensional reference model and the three-dimensional model, then the three-dimensional model was revisited to find the root cause of these differences and to take corrective action. During the modeling process, over 250 RELAP5-3D cases were created and analyzed, resulting in over 400 GB of system data. This section summarizes the results of only the final RELAP5-3D three-dimensional model, and compares several simulated parameters with the analogous one-dimensional reference model values.

5.1. Reactor Operating Parameters

The purpose of this section is to briefly compare several values for representative reactor parameters of the final three-dimensional model with the values for the same parameters of the one-dimensional reference model. Table 5.1 presents these parameters and the percent difference of the three-dimensional value with respect to the corresponding one-dimensional reference value, where the percent difference is simply the difference between the three-dimensional result and the one-dimensional result divided by the one-dimensional result.

Table 5.1. Comparison of the values from the final three-dimensional model with the values from the one-dimensional reference model for several important operating and design parameters.

Parameter Description	% Difference
Primary RCS Volume	0.00%
Total Hydrodynamic Volume	0.00%
NSSS Power	-0.03%
Reactor Power	0.00%
Thermal Design Flow Rate (total)	0.04%
Core Flow Rate	0.10%
Upper Bypass Flow Rate	0.35%
Core Bypass Flow Rate	-0.94%
Upper Bypass Fraction	0.31%
Core Bypass Fraction	-0.97%
Total Bypass Fraction	-0.74%
Coolant Pressure (Upper Plenum)	-0.11%
Primary Temp.- Vessel Outlet	-0.14%
Primary Temp.- Vessel Avg.	0.00%
Primary Temp.- Vessel Inlet	0.03%
Primary Temp.- Steam Gen. Outlet	0.03%
Steam Gen. Steam Outlet Temp.	0.04%
Steam Gen. Steam Outlet Pressure	0.17%
Steam Gen. Total Flow	0.18%
Steam Gen. Steam Outlet Quality	0.00%

The results from the three-dimensional nodalization show very little difference from the results of one-dimensional reference model. For the intended applications of this model, these differences (<1%) are not expected to be of great significance in the

final results. Additionally, the results of the final model are within published acceptability criteria for steady-state system simulations (Petruzzi & D'Auria, 2008). For example, these criteria state that bypass flow rates have an acceptable error of 10%, while the results performed here have an error of less than 1% from the one-dimensional reference model. While these results are satisfactory for the application here, they could be improved by further tuning of the RELAP5-3D input deck, if desired.

5.2. Local Reactor Coolant System Pressure

A second comparison of the three-dimensional model to the one-dimensional reference is in terms of local RCS pressure. In order for the model to be an appropriate representation of a PWR, the three-dimensional model should have similar pressure drops to the one-dimensional model. Table 5.2 provides the differences in the absolute pressures for several control volumes between the one-dimensional and three-dimensional models. For control volumes that have been re-nodalized in the three-dimensional model, the most representative control volume is used as an approximation instead (e.g. the middle ring of a cylindrical component). The locations of the control volumes can be obtained by referring to Fig. 3.1. The largest difference between the two models occurs at the core entry annulus region (50101). The large pressure in this control volume in the three-dimensional model is likely due to the representation of velocity in three coordinate directions. This node accepts flow radially inward and

redirects most of it axially downward, with a fraction of the flow instead flowing axially upward. The result of this may be that pressure is increased at the expense of what RELAP5-3D models as a loss of velocity; this is discussed in more detail in Section 3.1.11.4.3 of volume 1 of the RELAP5-3D manuals (RELAP5-3D Manuals, 2012). While some of these pressure differences appear high, the overall flow characteristics are very similar, with the possibility that much of the differences may be intrinsically due to the three-dimensional nodalization.

Table 5.2. Differences in the absolute pressure between control volumes of the final three-dimensional model and control volumes of the one-dimensional reference model.

Component Control Volume	**Description**	**Absolute Pressure Difference (psi)**
50101	Vessel Entry Annulus	8.68
58501	Upper Dome	-1.88
53501	Lower Plenum	-0.84
54501	Lower Core Plate	-0.31
84501	Upper Core Plate	1.16
11802	Cold Leg Exit	-0.15
11202	Crossover Leg Exit	-0.03
11301	RCS Pump Volume	-0.08
11601	Cold Leg Intermediate Node	-0.15
10001	Hot Leg Entry	0.00
10402	Hot Leg Exit	0.00
10601	Steam Generator Entrance	0.01
10801	Steam Generator U-Tube Entrance	0.01
10808	Steam Generator U-Tube Exit	-0.01
11001	Steam Generator Exit	-0.01

Other important aspects of the flow are the pressure differences between nodes of the system. Since the absolute pressures of the nodes presented are similar, it should be expected that the differential pressures between nodes are also similar. Several differential pressures are tabulated in Table 5.3 for both models, along with the differences between these values. The pressure drops show that, while the three-dimensional model is similar to the one-dimensional reference model, it is not identical to it. The differences in the pressure drops are small, but could be improved by more tweaking of the final model. Again, the intricacies of the three-dimensional model may lead to intrinsic differences between the two models. The pressure differences in the RCS loops remain very similar between the two models because these were not modified. Another source of error may be due to the final step of the modeling process. By reconstructing the reactor vessel component-by-component, each step requires the modification of both the new junctions created between two different three-dimensional components and temporary junctions between the newly added three-dimensional components and one-dimensional analogues. Thus it may be beneficial to add a "seventh" step to the modeling process in which the complete three-dimensional model is tweaked slightly to better agree with the one-dimensional reference.

Table 5.3. Comparison of the final three-dimensional model with the one-dimensional reference model with respect to the differential pressure between several control volumes.

Control Volume Pair	Description	Differential Pressure (psi)		
		1D Ref. Model	Final 3D Model	Difference
53501-11802	Vessel Entry and Downcomer	5.30	4.61	-0.69
58501-11802	Upper Plenum Bypass	-30.63	-32.36	-1.73
84501-54501	Core Pressure Drop	-27.52	-26.05	1.47
10001-84501	Core and Vessel Exit	-15.82	-16.98	-1.16
11202-11301	Pump Inlet	-46.36	-46.31	0.05
11301-11601	Pump Outlet	-23.14	-23.07	0.07
11601-11802	Cold Leg	0.49	0.49	0.00
10402-10001	Hot Leg	-1.00	-1.00	0.00
10601-10402	Stream Generator Inlet	4.72	4.72	0.00
10801-10601	U-Tubes Inlet	-6.18	-6.18	0.00
10808-10801	U-Tubes Pressure Drop	-19.58	-19.60	-0.02
11001-10808	U-Tubes Outlet	0.88	0.88	0.00
11202-11001	Steam Generator Outlet	-7.05	-7.06	-0.01

5.3. Temperature Profiles

Another important criterion for nuclear reactor safety analysis is fuel temperature. The one-dimensional reference model uses three unique heat structures to model the reactor core. The first heat structure simulates the average fuel channel (excluding the hottest fuel channel), the second simulates the hottest fuel channel, and the third simulates the hottest rod of the hottest fuel channel. The axial power profile was assumed to be equivalent to a typical power profile for a PWR at the end of the operational cycle.

The final three-dimensional model simulates all 193 fuel channels as separate heat structures. While it has the same axial profile as the one-dimensional model, it also has a lateral power profile. This power profile is simulated by using 45 unique assembly powers that form "quarter-core" symmetry. The assembly powers used in this model are illustrated in Fig. 5.1, where the coloring of each fuel channel represents the fraction of the power produced in that channel versus the total power of the reactor. The digits in selected cells will be used to characterize behavior in those channels later in this section.

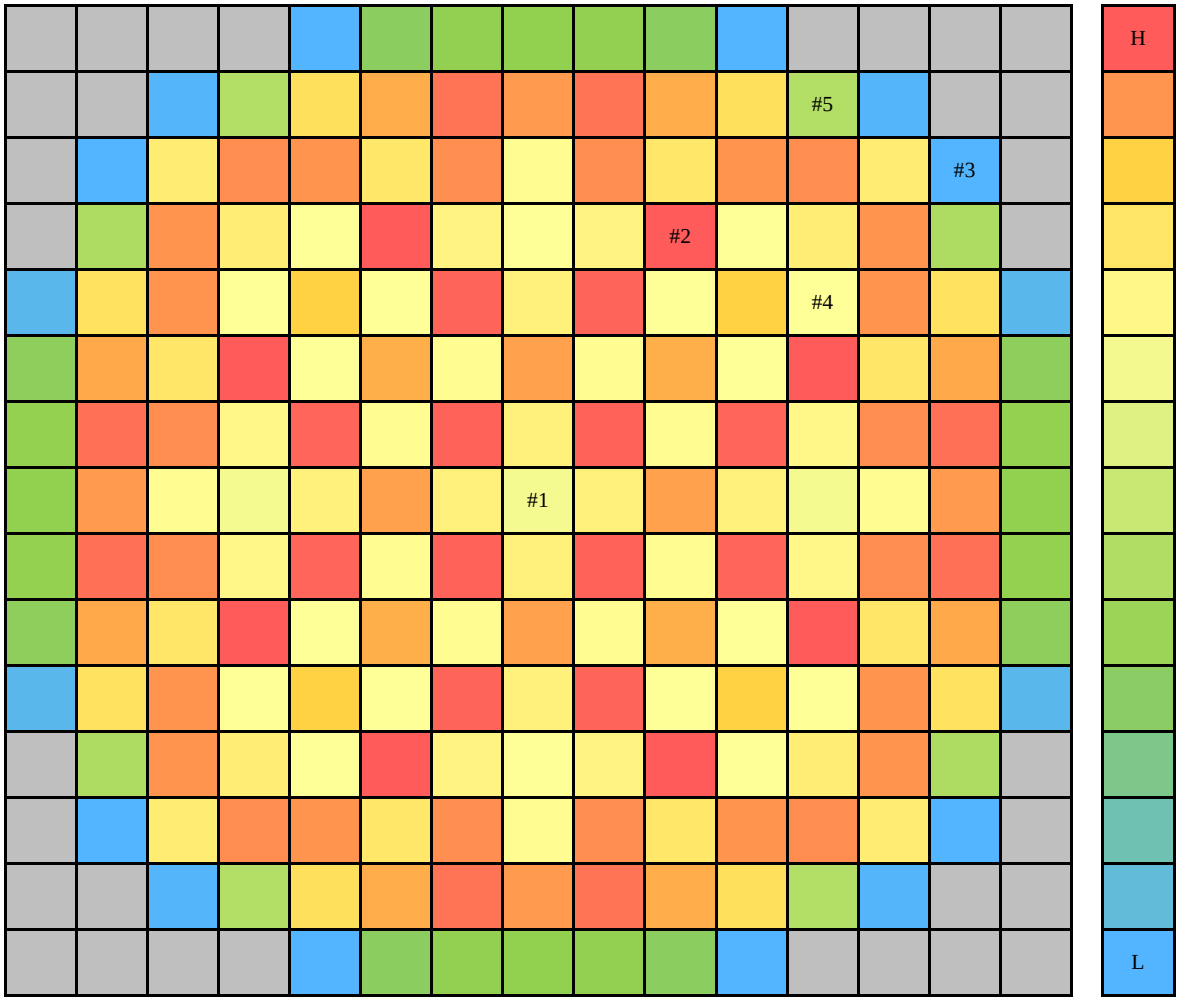

Figure 5.1. Illustration showing the relative assembly power coefficients used to create heat structures that produce a lateral power profile. Red and blue coloring correspond to high powers and low powers, as shown by the legend to the right.

It is fairly easy to illustrate the temperature distribution used in the one-dimensional reference model because there exists only one spatial variable and three heat structures. Figure 5.2 presents the fuel centerline temperature for the three heat structures of this model, while Fig. 5.3 illustrates the cladding surface temperature.

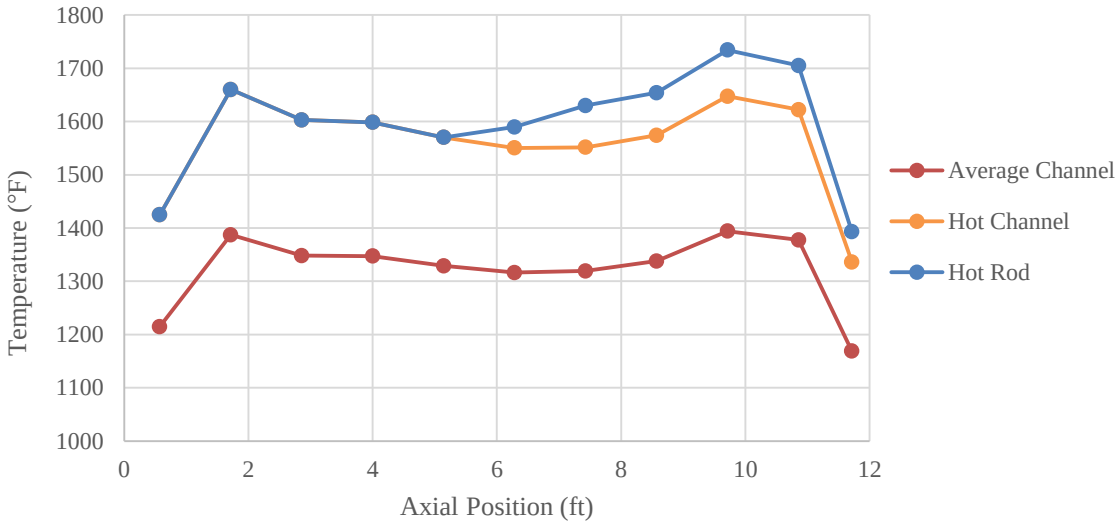

Figure 5.2. Fuel centerline temperature for the three heat structures of the one-dimensional reference model.

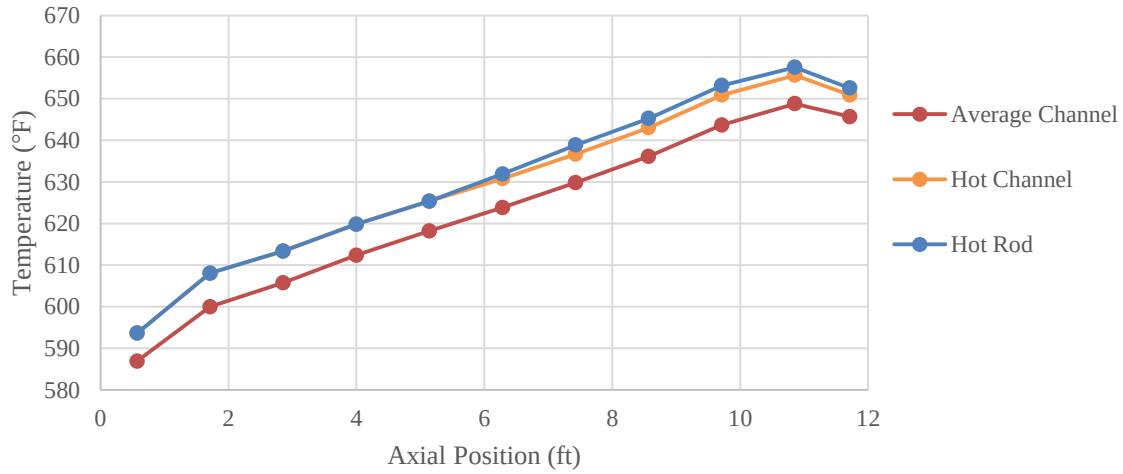

Figure 5.3. Fuel cladding temperature for the three heat structures of the one-dimensional reference model.

In order to compare the values from the three-dimensional model to the values from the one-dimensional reference model, individual heat structures must be selected and analyzed. In order to be concise and clear, five heat structures have been chosen that are representative of the core as a whole. These channels have been labeled in Fig. 5.1 for reference purposes. The first channel represents the central fuel assembly of the reactor, while the second and the third represent the highest and lowest power coefficients, respectively. The fourth channel was selected because it has a power coefficient very close to unity, so it should produce a similar amount of power to the average fuel channel power from the one-dimensional model, after normalization. Lastly, the fifth channel was selected because its coefficient was an intermediary of the other selected channel power coefficients. Figure 5.4 illustrates the fuel centerline temperatures for these five heat structures as a function of axial position. Figure 5.5 presents the fuel cladding surface temperature for these five heat structures. While these figures relate different heat structures from the three-dimensional model to each other, a direct comparison of the average and hot channels of the one-dimensional model to channels number #4 and #2 of the three-dimensional model is also performed. Figure 5.6 provides this comparison for fuel centerline temperature, while Fig. 5.7 provides this comparison for fuel cladding temperature.

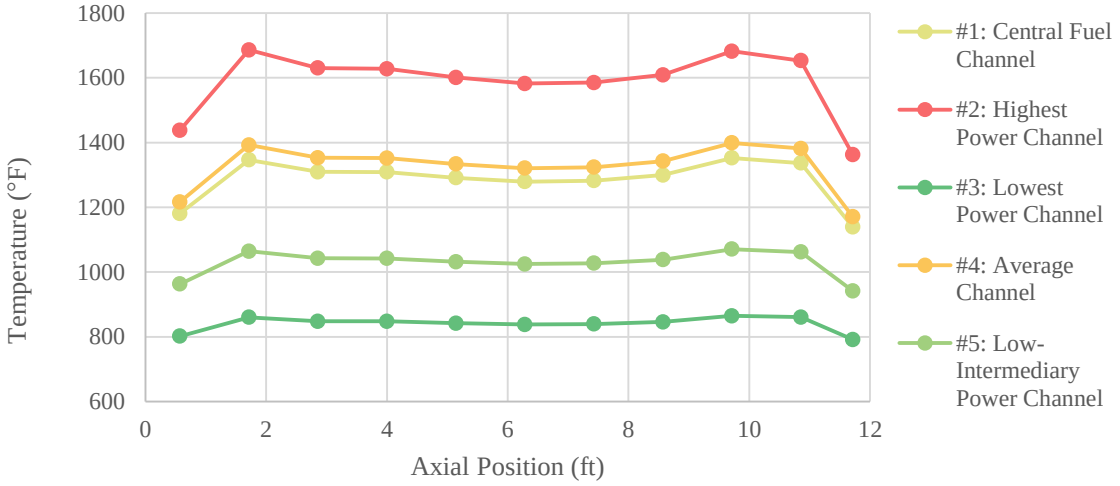

Figure 5.4. Fuel centerline temperatures for the five representative heat structures of the final three-dimensional model as a function of axial position.

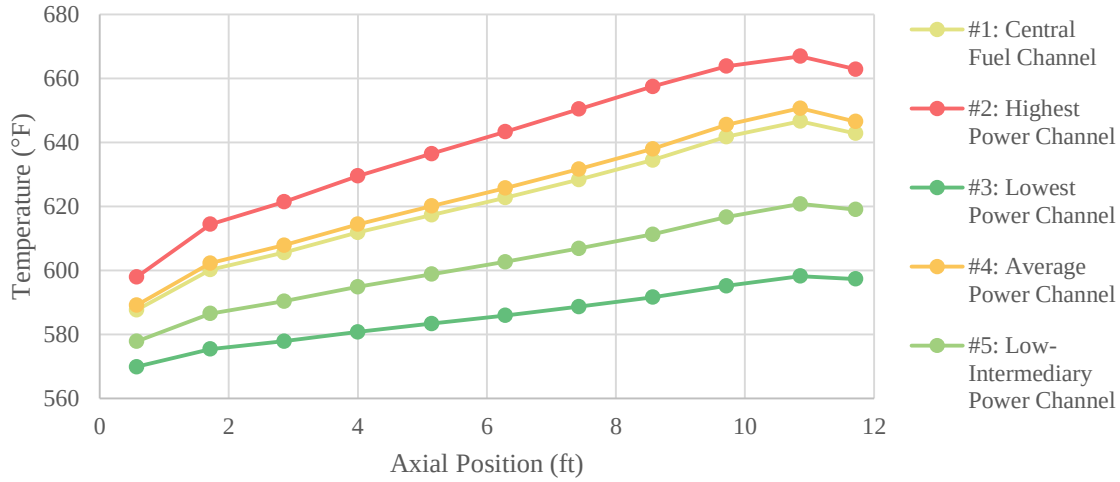

Figure 5.5. Fuel cladding temperatures for the five representative heat structures of the final three-dimensional model as a function of axial position.

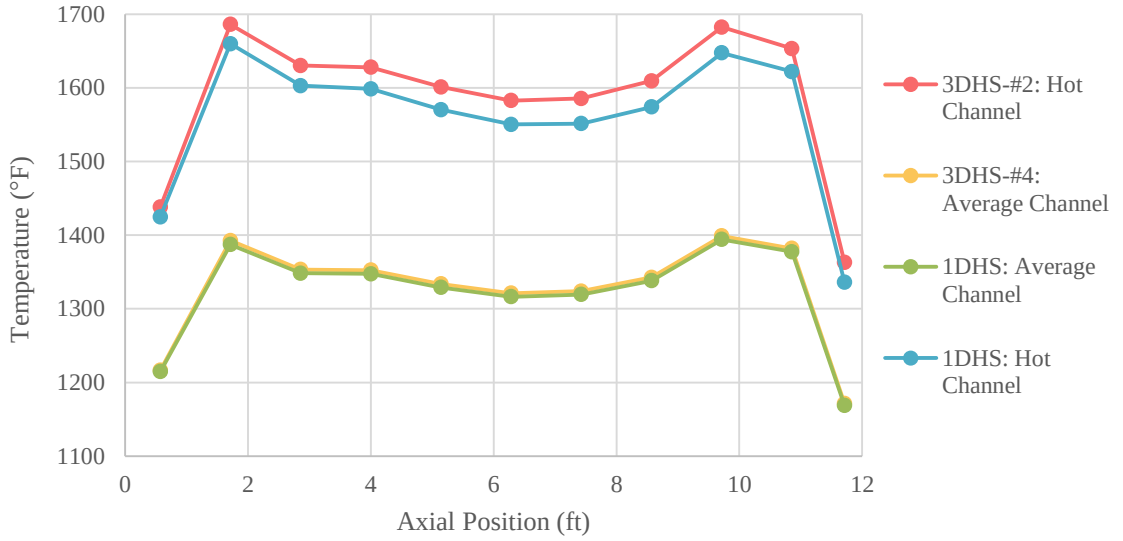

Figure 5.6. Fuel centerline temperatures for two heat structures from the three-dimensional model and their nearest analogues from the one-dimensional model.

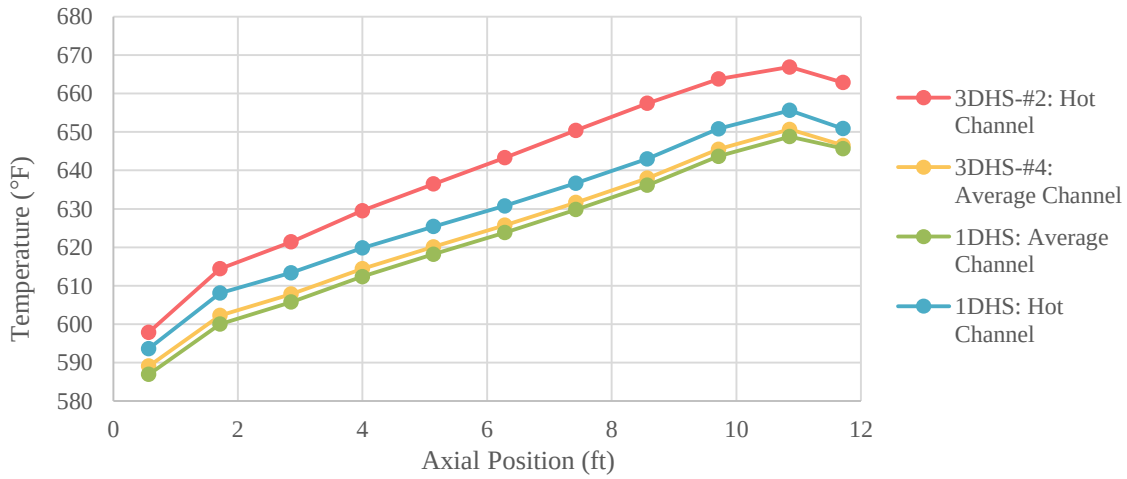

Figure 5.7. Fuel cladding temperatures for two heat structures from the three-dimensional model and their nearest analogues from the one-dimensional model.

These figures illustrate the consistency of the three-dimensional model with the one-dimensional model. For example, a comparison of the fuel channel with an assembly power near unity in the three-dimensional model with the average assembly from the one-dimensional reference model shows that both fuel centerline and fuel cladding temperatures are approximately equal as a function of axial position. For the hottest assemblies in the three-dimensional and one-dimensional models, there is some disagreement. Part of this disagreement is due to different power coefficients in the RELAP5-3D input decks. The lateral power profile that was chosen for the three-dimensional model leads to some differences between the two models, but there may exist other sources for this discrepancy.

Thus far, only fuel centerline and cladding temperatures have been discussed. In order to complete this discussion, an examination of coolant temperatures and coolant velocities should also be performed. In the one-dimensional model, the core was modeled using a single hydrodynamic component with 21 axial control volumes. This means that all of the heat structures from the one-dimensional model share the same boundary conditions – those defined by the 21 axial control volumes. In the three-dimensional model, each heat structure node was interfaced with a single, unique hydrodynamic control volume, resulting in unique but coupled boundary conditions for each heat structure. Figure 5.8 presents the coolant temperature as a function of axial position for the different control volumes, while Fig. 5.9 does the same with coolant velocities. These are not the only changes to the reactor coolant within the reactor core;

the density of the coolant decreases as heat is added, the pressure decreases as elevation increases and friction and form losses accumulate, and flow behavior changes according to natural laws. The hydrodynamic control volumes presented in these figures are interfaced with the same set of heat structures that were used for fuel centerline and cladding temperatures.

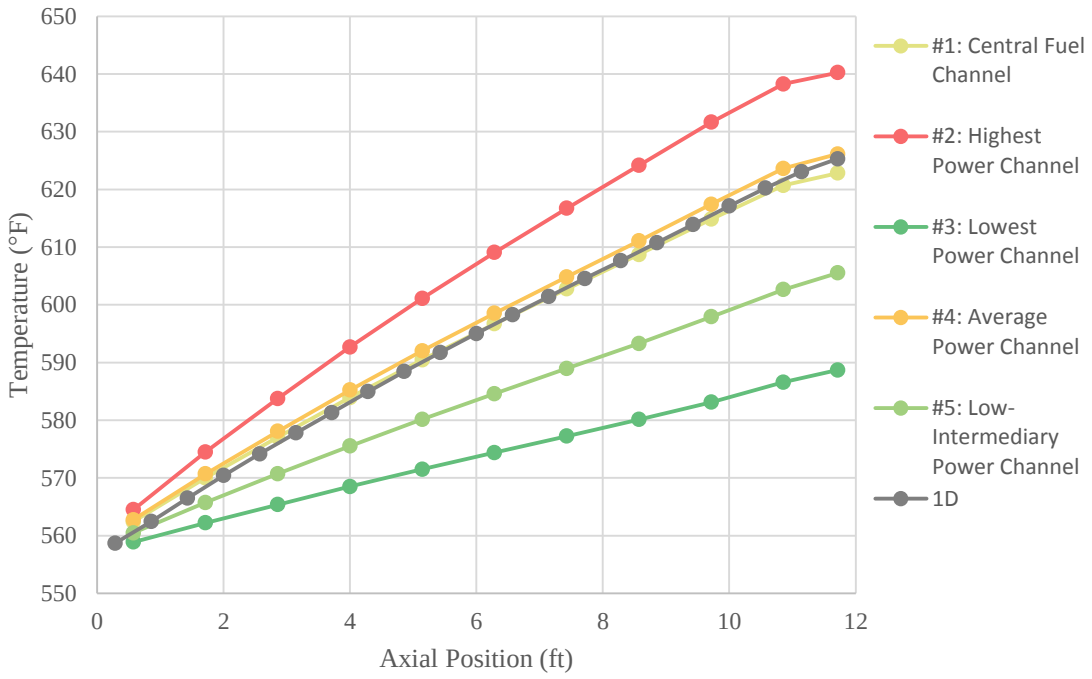

Figure 5.8. Reactor coolant temperatures in control volumes interfaced with selected heat structures as a function of axial position from core entry.

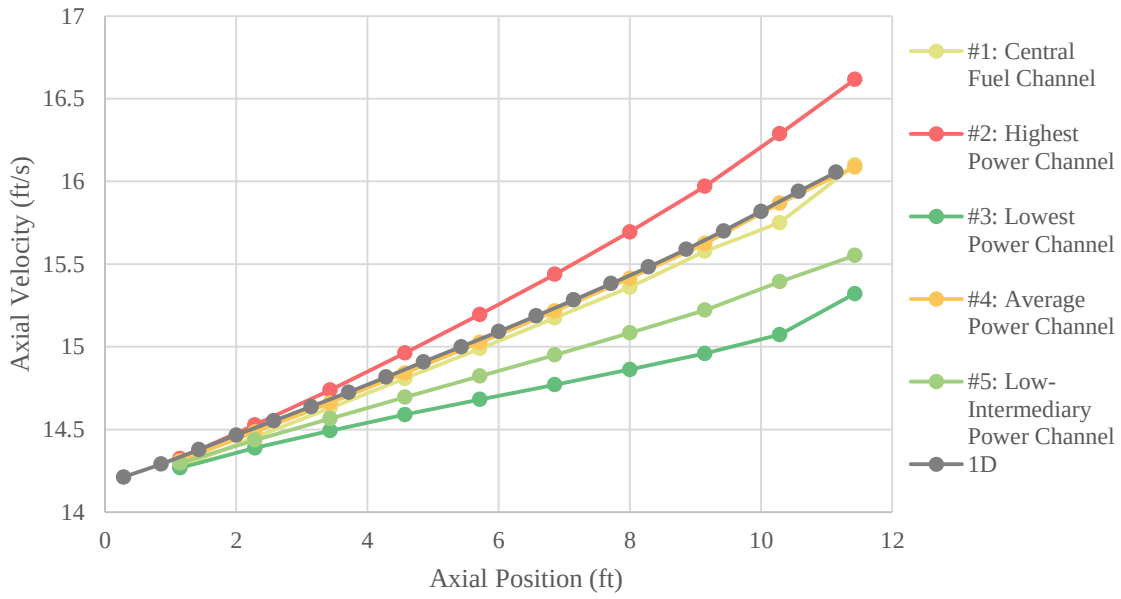

Figure 5.9. The axial components for reactor coolant velocities in the control volumes interfaced with selected heat structures as a function of axial position from core entry.

These figures help to illuminate the sources of the discrepancies found, especially those occurring between the hottest channels of the three-dimensional and one-dimensional models. Since the heat structure representing the hottest channel in the one-dimensional model is connected to the same control volumes as the heat structure representing the average channel, it shares the same boundary conditions. This translates to coolant temperatures that are lower than those obtained in the three-dimensional simulation for the hottest heat structures, as shown in Fig. 5.8. Conversely, the three-dimensional model has unique hydrodynamic control volumes for each heat structure node. While these control volumes are all connected such that flow can occur

between them, there are significant friction and form losses that the flow must overcome. This results in a heterogeneity in the reactor coolant throughout the reactor core volume. The final comparison will be focused on the total heat transfer coefficient, h, which can be related to the heat flux using Eq. 5.1, where q'' is the heat flux from the heat structure to the coolant, T_{Cl} is the cladding temperature, and T_{Co} is the coolant temperature (Todreas & Kazimi, 2012).

$$q'' = h(T_{Cl} - T_{Co}) \tag{5.1}$$

The total heat transfer coefficient is presented for selected flow channels as a function of axial position in Fig. 5.10. The flow channels selected are those with the highest, lowest, and "approximately average" power fractions from the three-dimensional model, as well as the heat structures corresponding to the average and hottest channels in the one-dimensional model. This plot shows that the hottest channels in both models experience a rise in the heat transfer coefficient as the coolant approaches the core exit. This is largely caused by a change in the heat transfer mechanism, or 'mode.' RELAP5-3D uses discrete heat transfer modes to calculate the heat transfer coefficient for convective heat transfer. While most of the heat structures of both models use a "single-phase liquid convection, subcooled wall, low void fraction" mode, the hotter heat structures experience a "subcooled nucleate boiling" heat transfer mode. This results in more efficient heat transfer as shown by the results from Fig. 5.10 and the

relationship presented as Eq. 5.1. While both the one-dimensional and the three-dimensional model experience this change of heat transfer modes at certain nodes, the change is more pronounced and results in a much larger change in the heat transfer coefficient in the three-dimensional model. This is due to the effects of heterogeneity and the boundary conditions already discussed.

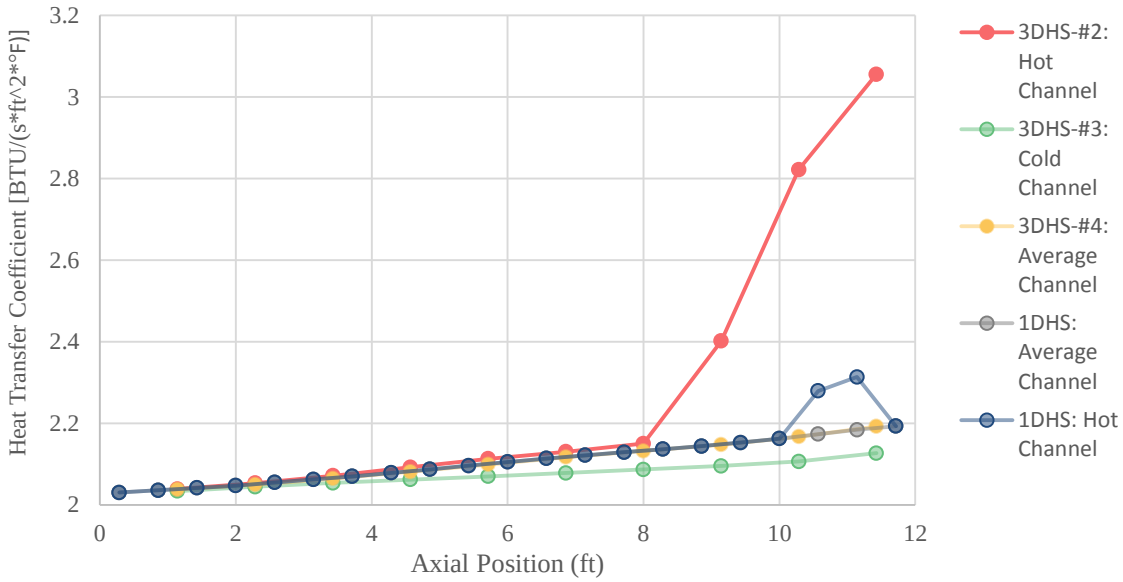

Figure 5.10. Heat transfer coefficient for selected heat structures from the one-dimensional and three-dimensional models as a function of axial position.

By taking into consideration the spatial heterogeneity present in the three-dimensional model (both in terms of fluid and heat structures), the discrepancies between the one-dimensional reference model and the three-dimensional model can be explained.

6. CONCLUSIONS

A typical PWR was successfully modeled using three-dimensional components in the RELAP5-3D thermal hydraulics system analysis code. RELAP5-3D was chosen due to its reputation in the nuclear safety industry as well as its successful use in similar works. It was determined that RELAP5-3D is sufficient for modeling several phenomena associated with LOCA scenarios, including those postulated in GSI-191.

Before constructing the three-dimensional model, a simpler one-dimensional model was used as a reference. This model created the baseline or foundation for the more complicated three-dimensional model both in terms of input modeling and output results. Several components within the reactor vessel were transformed from one-dimensional representations to three-dimensional representations. In order to perform these transformations, analysis was required to ensure consistency with the one-dimensional reference. After the creation of an initial three-dimensional model that was analogous to the one-dimensional reference, the three-dimensional model was adjusted to save on computational time and resources. This was accomplished by lowering the Courant time step and by consolidating unnecessary nodes and junctions. The geometry of the model was then adjusted to more accurately represent typical PWRs, and to fully utilize the benefits of three-dimensional component nodalization. Next, any abnormalities of the model were resolved, and the input deck was adjusted to increase robustness and soundness of the model. Lastly, the model was adjusted to produce

steady-state results that were similar to the results from the one-dimensional reference model. This was performed by reconstructing the three-dimensional model by replacing one-dimensional components one at a time, comparing the results from these intermediate models, and adjusting the RELAP5-3D input deck to account for any differences caused by the new nodalizations.

As part of the model development process, a tool to calculate the adjoining area for multiple junction cards was created. The tool input, output, and implementation was discussed, and a summary of tool verification and validation efforts was provided. It was determined that use of this tool added robustness to the methodology while increasing the accuracy and efficiency of the modeling efforts in comparison to efforts that would be undertaken in the absence of such a tool.

Lastly, the results from the final steady-state three-dimensional model were reported, along with those of the one-dimensional reference model. These results are consistent with each other and with those of a typical PWR. While the modeling process may be arduous, the care and techniques involved produce results that are sufficient for safety analyses. If even more similarity between the two models is desired, it can be obtained by further tweaking the final three-dimensional model.

REFERENCES

Fletcher, C., Bayless, P., Davis, C., & et.al. (1997). *Adequacy Evaluation of RELAP5/MOD3, Version 3.2.1.2 for Simulating AP600 Small Break Loss-of-Coolant Accidents.* INEEL/NRC.

Idaho National Laboratory. (2014, May 15). *About RELAP5-3D.* Retrieved from www.inl.gov/relap5/relap5doc/relap5doe.doc

Knowledge Center. (2014, May). Retrieved from Nuclear Energy Institute: http://www.nei.org/Knowledge-Center/Nuclear-Statistics/World-Statistics

Kovtonyuk, A., Petruzzi, A., Parisi, C., & D'Auria, F. (2008). RELAP5-3D Analysis of OECD-NEA/NRC BFBT Benchmark. *16th International Conference on Nuclear Engineering.* Orlando, FL.

Los Alamos National Laboratory. (2002). *NUREG/CR-6770-GSI-191: Themal-Hydraulic Response of PWR Reactor Coolant System and Containments ot Selected Accident Sequences.*

Magnusson, R. (2013). *Modeling of PWR LOCA Experiments in RELAP5 Based on PREMIUM Benchmark.* Chalmers University of Technology. Gothenburg, Sweden.

Petruzzi, A., & D'Auria, F. (2008). Thermal-Hydraulic System Codes in Nuclear Reactor Safety and Qualification Procedures. *Science and Technology of Nuclear Installations*.

RELAP5-3D Manuals. (2012). Retrieved from Idaho National Laboratory: http://www.inl.gov/relap5/r5manuals.htm

Rodriguez, O. A. (2012). *RELAP5-3D Thermal Hydraulics Computer Program Analysis Coupled with Dakota and STAR-CCM+ Codes.* Texas A&M University. College Station, TX.

Roux, V. J.-P. (2001). *Evaluation of RELAP5 Reactor Core Modeling Capability.* University of Florida. Gainesville, FL.

Standards Coordination Committee of the IEEE Computer Society. (1990). *IEEE Standard Computer Dictionary: A Compilation of IEEE Standard Computer Glossaries (610).* New York.

Todreas, N. E., & Kazimi, M. S. (2012). *Nuclear Systems: Volume 1.* Boca Raton: CRC Press.

Vaghetto, R., & Hassan, Y. A. (2013). Study of debris-generated core blockage scenarios during loss of coolant accidents using RELAP5-3D. *Nuclear Engineering and Design*, 144-155.